International Journal of Heat and Mass Transfer 55 (2012) 3246–3261

Contents lists available at SciVerse ScienceDirect

International Journal of Heat and Mass Transfer

journal homepage: www.elsevier.com/locate/ijhmt

Universal approach to predicting two-phase frictional pressure drop for adiabatic and condensing mini/micro-channel flows

Sung-Min Kim, Issam Mudawar *

Boiling and Two-Phase Flow Laboratory (BTPFL), Purdue University International Electronic Cooling Alliance (PUIECA), Mechanical Engineering Building, 585 Purdue Mall, West Lafayette, IN 47907-2088, USA

ARTICLE INFO

Article history:
Received 13 January 2012
Received in revised form 2 February 2012
Accepted 15 February 2012
Available online 28 March 2012

Keywords:
Pressure drop
Adiabatic two-phase flow
Condensation
Mini-channel
Micro-channel

ABSTRACT

Previous models and correlations for the prediction of pressure drop in adiabatic and condensing mini/micro-channel flows have been validated for only a few working fluids and relatively narrow ranges of relevant parameters. A universal predictive approach for these flows must be capable of tackling many fluids with drastically different thermophysical properties and very broad ranges of all geometrical and flow parameters of practical interest. To achieve this goal, a new consolidated database of 7115 frictional pressure gradient data points for both adiabatic and condensing mini/micro-channel flows is amassed from 36 sources. The database consists of 17 working fluids, hydraulic diameters from 0.0695 to 6.22 mm, mass velocities from 4.0 to 8528 kg/m^2 s, liquid-only Reynolds numbers from 3.9 to 89,798, flow qualities from 0 to 1, and reduced pressures from 0.0052 to 0.91. It is shown that, while a few prior models and correlations provide fair predictions of the consolidated database, their predictive accuracy is highly compromised for certain subsets of the database. A universal approach to predicting two-phase frictional pressure drop is proposed by incorporating appropriate dimensionless relations in a separated flow model to account for both small channel size and different combinations of liquid and vapor states. This approach is shown to provide excellent predictions of the entire consolidated database and fairly uniform accuracy against all parameters of the database. This approach is also capable of tackling single and multiple channels as well as situations involving significant flow deceleration due to condensation.

© 2012 Elsevier Ltd. All rights reserved.

1. Introduction

Advances in many modern technologies are facing unprecedented challenges stemming from the need to remove large, highly concentrated heat loads. In applications such as high performance computers, electrical vehicle power electronics, avionics, and directed energy laser and microwave weapon systems, there has been a fairly steady rise in heat dissipation per unit volume at both the device and system levels [1,2]. Phase change cooling schemes are ideally suited for these applications, given their ability to deliver orders of magnitude enhancement in boiling and condensation heat transfer coefficients. This attribute has led to a surge in the number of published studies addressing means for capitalizing on the cooling merits of phase change using a variety of configurations, including spray [3–5], jet [6–9], and micro-channel cooling schemes [2,10–13], as well as techniques to enhance surface micro-structure [14].

Condensers utilizing mini/micro-channels are especially suited for applications demanding high heat dissipation in a limited volume. These condensers maintain mostly annular flow to take advantage of the large condensation heat transfer coefficients associated with thin liquid films. A very thin film is initiated in the upstream region of the channel, driven by shear stresses exerted by the vapor core. Decreasing the channel diameter increases both vapor velocity and the interfacial shear stress, which causes a thinning of the annular film and increases the condensation heat transfer coefficient. As the vapor is gradually converted to liquid, the film thickness increases along the micro-channel, which eventually leads to a collapse of the annular regime and successive formation of slug, bubbly, and liquid flow regimes.

Unfortunately, the heat transfer benefits of decreasing the channel diameter are realized at the expense of higher pressure drop, which may adversely influence the overall efficiency of a two-phase system. Therefore, the design of high performance mini/micro-channel condensers requires accurate predictive tools for both pressure drop and condensation heat transfer coefficient. The present study concerns pressure drop prediction.

Recently, the authors of the present study [15] examined the predictive accuracy of mini/micro-channel separated flow pressure

* Corresponding author. Tel.: +1 765 494 5705; fax: +1 765 494 0539.
E-mail address: mudawar@ecn.purdue.edu (I. Mudawar).
URL: https://engineering.purdue.edu/BTPFL (I. Mudawar).

0017-9310/$ - see front matter © 2012 Elsevier Ltd. All rights reserved.
doi:10.1016/j.ijheatmasstransfer.2012.02.047

Nomenclature

Bo	Bond number
*Bo**	modified Bond number
C	parameter in Lockhart–Martinelli model
Ca	Capillary number
D	tube diameter
D^h	hydraulic diameter
Fr	Froude number
f	Fanning friction factor
G	mass velocity
g	gravitational acceleration
Ga	Galileo number
J	superficial velocity
L	length
MAE	mean absolute error
N	number of data points
N^{conf}	Confinement number
P	pressure
P^{crit}	critical pressure
P^R	reduced pressure, $P_R = P/P_{crit}$
ΔP	pressure drop
Re	Reynolds number
Su	Suratman number
u	mean velocity
v	specific volume
v^{fg}	specific volume difference between saturated vapor and saturated liquid
We	Weber number
X	Lockhart–Martinelli parameter
x	thermodynamic equilibrium quality
z	stream-wise coordinate

Greek symbols

α	void fraction
β	channel aspect ratio ($\beta < 1$)
θ	percentage predicted within ±30%
λ	mean absolute error
μ	dynamic viscosity
ξ	percentage predicted within ±50%
ρ	density
$\bar{\rho}$	mixture density
σ	surface tension
ϕ	two-phase multiplier; channel inclination angle

Subscripts

A	accelerational
exp	experimental (measured)
F	frictional
f	saturated liquid
fo	liquid only
G	gravitational
g	saturated vapor
go	vapor only
k	liquid (*f*) of vapor (*g*)
pred	predicted
sat	saturation
tp	two-phase
tt	turbulent liquid–turbulent vapor
tv	turbulent liquid–laminar vapor
vt	laminar liquid–turbulent vapor
vv	laminar liquid–laminar vapor

drop correlations and concluded that, on a local basis, mini/micro-channel condensing flow is closer in flow structure to adiabatic two-phase flow than boiling flow. As illustrated in Fig. 1, one obvious difference between flow boiling on one hand, and condensing and adiabatic two-phase flows on the other, is the relative abundance of entrained droplets in the former and absence from the latter two. This phenomenon is especially important for mini/micro-channel flows, where the annular regime is dominant regardless of heating conditions. As indicated by Qu and Mudawar [16], the transition to the annular regime in flow boiling occurs far upstream in a micro-channel, with an abundance of entrained droplets formed by shattering of liquid from the micro-channel's upstream. However, recent video imaging results show no droplets are formed in the annular condensation region of a micro-channel [15]. These obvious differences suggest that different pressure drop predictive tools be developed for condensing and adiabatic flows on one hand compared to those for boiling flow.

Studies on two-phase adiabatic and condensing flows in mini/micro-channels [17–52] have resulted in different approaches to predicting pressure drop. The vast majority of studies concerning two-phase pressure drop prediction are based on the homogeneous equilibrium model [53–59] or semi-empirical correlations [21,39,60–70]. However, these methods have been validated only for specific flow configurations and relatively narrow ranges of operating conditions. Of the different condensation regimes, annular flow is accurately modeled by the control-volume-based approach. This approach proved highly effective in predicting a variety of complex two-phase flow configurations including pool boiling [71,72], and vertical separated flow boiling along short walls [73,74] and long heated walls [75–78]. Recently, the authors of the present study used the control volume approach to construct a new model for annular condensation in mini/micro-channels

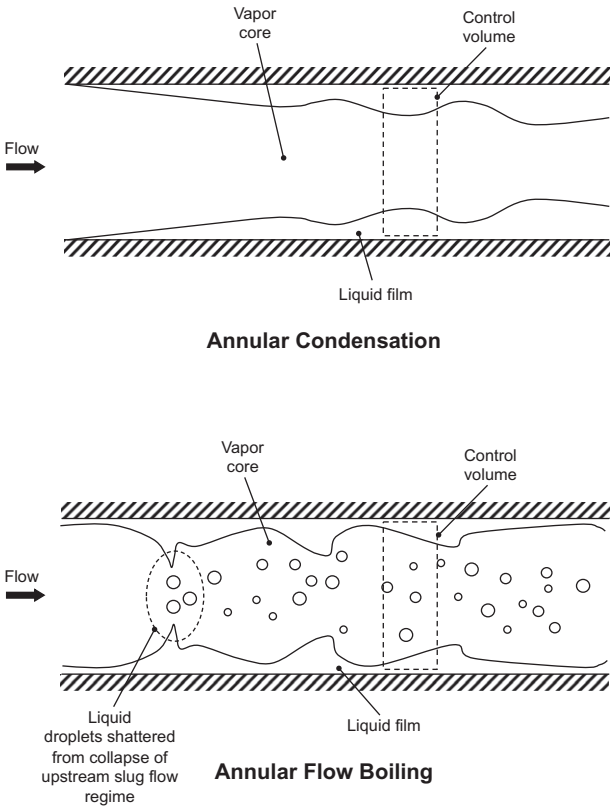

Fig. 1. Fundamental differences between annular condensation (also annular adiabatic flow, on a local basis) and annular flow boiling in mini/micro-channels [15].

[79]. Unlike this latter study, the primary objective of the present study is to develop a generalized predictive tool for pressure drop in both adiabatic and condensing mini/micro-channel flows applicable to all condensation regimes.

Table 1
Two-phase mixture viscosity models employed in the homogeneous equilibrium model.

Author(s)	Equation
McAdams et al. [53]	$\frac{1}{\mu_{tp}} = \frac{x}{\mu_g} + \frac{1-x}{\mu_f}$
Akers et al. [54]	$\mu_{tp} = \frac{\mu_f}{\left[(1-x)+x\left(\frac{v_g}{v_f}\right)^{0.5}\right]}$
Cicchitti et al. [55]	$\mu_{tp} = x\mu_g + (1-x)\mu_f$
Owens [56]	$\mu_{tp} = \mu_f$
Dukler et al. [57]	$\mu_{tp} = \frac{x v_g \mu_g + (1-x) v_f \mu_f}{x v_g + (1-x) v_f}$
Beattie and Whalley [58]	$\mu_{tp} = \omega\mu_g + (1-\omega)(1+2.5\omega)\mu_f$ $\omega = \frac{x v_g}{v_f + x v_{fg}}$
Lin et al. [59]	$\mu_{tp} = \frac{\mu_f \mu_g}{\mu_g + x^{1.4}(\mu_f - \mu_g)}$

Only a few studies have been published that address the development of a generalized correlation for two-phase frictional pressure drop for mini/micro-channels [68–70]. But what is still lacking is a predictive tool that is applicable to a wide range of working fluids, mass velocities, pressures (atmospheric to near-critical pressures), and channel diameters (tens of micrometers to a few millimeters). As discussed in Ref. [2], the development of this predictive tool is the primary motivation for a series of studies that have been recently initiated at the Purdue University Boiling and Two-Phase Flow Laboratory (PU-BTPFL), including the present study, to (1) consolidate world databases for condensation and flow boiling in mini/micro-channels, and (2) develop predictive approaches for both pressure drop and heat transfer coefficient. The approach used here follows closely the methodology adopted in a previous series of studies at PU-BTPFL addressing the prediction of flow boiling critical heat flux (CHF) [80–83].

Most of the published works recommended for the prediction of micro/micro-channel pressure drop [39,63,64,66,68–70] are based on the Lockhart–Martinelli [60] method. To account for the influence of small channel diameter on pressure drop, the parameter C of the Lockhart–Martinelli model, whose magnitude depends on a

Table 2
Two-phase frictional pressure gradient correlations.

Author(s)	Equation	Remarks
Lockhart and Martinelli [60]	$\left(\frac{dP}{dz}\right)_F = \left(\frac{dP}{dz}\right)_f \phi_f^2,\ \phi_f^2 = 1 + \frac{C}{X} + \frac{1}{X^2},\ X^2 = \frac{(dP/dz)_f}{(dP/dz)_g}$ C_{vv} = 5, C_{tv} = 10, C_{vt} = 12, C_{tt} = 20	D_h = 1.49–25.83 mm, adiabatic, water, oils, hydrocarbons
Friedel [61]	$\left(\frac{dP}{dz}\right)_F = \left(\frac{dP}{dz}\right)_{fo} \phi_{fo}^2$ $\phi_{fo}^2 = (1-x)^2 + x^2\left(\frac{v_g}{v_f}\right)\left(\frac{f_{go}}{f_{fo}}\right) + 3.24x^{0.78}(1-x)^{0.224}\left(\frac{v_g}{v_f}\right)^{0.91}\left(\frac{\mu_g}{\mu_f}\right)^{0.19}\left(1-\frac{\mu_g}{\mu_f}\right)^{0.7} Fr_{tp}^{-0.045} We_{tp}^{-0.035}$ $Fr_{tp} = \frac{G^2}{g D_h \rho_H^2},\ We_{tp} = \frac{G^2 D_h}{\sigma \rho_H},\ \rho_H = \frac{1}{x v_g + (1-x) v_f}$	D > 4 mm, air–water, air–oil, R12 (25,000 data points)
Muller-Steinhagen and Heck [62]	$\left(\frac{dP}{dz}\right)_F = \left\{\left(\frac{dP}{dz}\right)_{fo} + 2\left[\left(\frac{dP}{dz}\right)_{go} - \left(\frac{dP}{dz}\right)_{fo}\right]x\right\}(1-x)^{1/3} + \left(\frac{dP}{dz}\right)_{go} x^3$	D = 4–392 mm, air–water, water, hydrocarbons, refrigerants (9300 data points)
Mishima and Hibiki [64]	$\left(\frac{dP}{dz}\right)_F = \left(\frac{dP}{dz}\right)_f \phi_f^2,\ \phi_f^2 = 1 + \frac{C}{X} + \frac{1}{X^2}$ For rectangular channel, $C = 21[1 - exp(-0.319 D_h)]$; D_h[mm] For circular tube, $C = 21[1 - exp(-0.333 D)]$; D[mm]	D = 1.05–4.08 mm, adiabatic, air–water
Wang et al. [63]	For $G \geqslant 200$ kg/m^{2}s $\left(\frac{dP}{dz}\right)_F = \left(\frac{dP}{dz}\right)_g \phi_g^2,\ \phi_g^2 = 1 + 9.4X^{0.62} + 0.564X^{2.45}$ For $G < 200$kg/m^{2}s, $\left(\frac{dP}{dz}\right)_F = \left(\frac{dP}{dz}\right)_f \phi_f^2,\ \phi_f^2 = 1 + \frac{C}{X} + \frac{1}{X^2}$ $C = 4.566 \times 10^{-6} X^{0.128} Re_{fo}^{0.938}\left(\frac{v_f}{v_g}\right)^{2.15}\left(\frac{\mu_f}{\mu_g}\right)^{5.1}$	D = 6.5 mm, adiabatic, R22, R134a, R407C
Yang and Webb [21]	$\left(\frac{dP}{dz}\right)_F = -0.87 Re_{eq}^{0.12} f_{fo} \frac{G_{eq}^2 v_f}{D_h},\ Re_{eq} = G\left[(1-x) + x\left(\frac{\rho_f}{\rho_g}\right)^{0.5}\right]\frac{D_h}{\mu_f}$	D_h = 1.56, 2.64 mm, adiabatic, R12, Re_{fo} > 2500
Yan and Lin [65]	$\left(\frac{dP}{dz}\right)_F = -996.6 Re_{eq}^{-1.074} \frac{G_{eq}^2 v_f}{D_h}$	D = 2.0 mm, condensation, R134a, Re_{eq} > 2000
Lee and Lee [66]	$\left(\frac{dP}{dz}\right)_F = \left(\frac{dP}{dz}\right)_f \phi_f^2 \phi_f^2 = 1 + \frac{C}{X} + \frac{1}{X^2},\ \psi = \frac{\mu_f j_f}{\sigma},\ \lambda = \frac{\mu_f^2}{\rho_f \sigma D_h}$ $C_{vv} = 6.833 \times 10^{-8} \lambda^{-1.317} \psi^{0.719} Re_{fo}^{0.557},\ C_{tv} = 3.627 Re_{fo}^{0.174}$ $C_{vt} = 6.185 \times 10^{-2} Re_{fo}^{0.726},\ C_{tt} = 0.048 Re_{fo}^{0.451}$	D_h = 0.78–6.67 mm, adiabatic, air–water
Chen et al. [67]	$\left(\frac{dP}{dz}\right)_F = \left(\frac{dP}{dz}\right)_{fo,Friedel}\Omega,\ Bo* = g(\rho_f - \rho_g)\frac{(D_h/2)^2}{\sigma}$ For $Bo* < 2.5\Omega = \frac{0.0333 Re_{fo}^{0.45}}{Re_g^{0.09}(1+0.4e^{-Bo*})}$ For $Bo* \geqslant 2.5\Omega = \frac{We_{tp}^{0.2}}{(2.5+0.06 Bo*)}$	D = 1.02–9 mm, adiabatic, air–water, R410A, ammonia
Hwang and Kim [39]	$\left(\frac{dP}{dz}\right)_F = \left(\frac{dP}{dz}\right)_f \phi_f^2,\ \phi_f^2 = 1 + \frac{C}{X} + \frac{1}{X^2},\ C = 0.227 Re_{fo}^{0.452} X^{-0.32} N_{conf}^{-0.82}$	D = 0.244, 0.430, 0.792 mm, adiabatic, R134a, Re_{fo} < 2000
Sun and Mishima [68]	$\left(\frac{dP}{dz}\right)_F = \left(\frac{dP}{dz}\right)_f \phi_f^2,\ \phi_f^2 = 1 + \frac{C}{X} + \frac{1}{X^2},\ C = 1.79\left(\frac{Re_g}{Re_f}\right)^{0.4}\left(\frac{1-x}{x}\right)^{0.5}$	D_h = 0.506–12 mm, air–water, refrigerants, CO_2 (2092 data points)
Li and Wu [69]	$\left(\frac{dP}{dz}\right)_F = \left(\frac{dP}{dz}\right)_f \phi_f^2,\ \phi_f^2 = 1 + \frac{C}{X} + \frac{1}{X^2}$ For $Bo \leqslant 1.5, C = 11.9 Bo^{0.45}$ For $1.5 < Bo \leqslant 11, C = 109.4(Bo Re_f^{0.5})^{-0.56}$	D_h = 0.148–3.25 mm, adiabatic, refrigerants, ammonia, propane, nitrogen (769 data points)
Zhang et al. [70]	$\left(\frac{dP}{dz}\right)_F = \left(\frac{dP}{dz}\right)_f \phi_f^2,\ \phi_f^2 = 1 + \frac{C}{X} + \frac{1}{X^2}$ For adiabatic liquid–gas flow, $C = 21[1 - exp(-0.674/N_{conf})]$ For adiabatic liquid–vapor flow, $C = 21[1 - exp(-0.142/N_{conf})]$	D_h = 0.07–6.25 mm, adiabatic, air/N_2–water, air/ethanol, refrigerants, ammonia, water (2201 data points), not recommended for turbulent liquid–turbulent vapor (tt) flow

combination of possible vapor and liquid laminar/turbulent flow states, is replaced by a function of relevant dimensionless groups.

In the present study, published pressure drop databases for both adiabatic and condensing mini/micro-channel flows are amassed from 36 sources. The data are compared to predictions of previous homogeneous equilibrium models, and semi-empirical correlations for both macro-channels and mini/micro-channels. A new generalized correlation for two-phase frictional pressure drop is derived that is proven capable of predicting the data for very broad ranges of operating conditions and many working fluids with high accuracy.

2. Previous predictive two-phase pressure drop methods

The two-phase pressure drop can be expressed as the sum of frictional, gravitational and accelerational (or decelerational) components,

$$\Delta P_{tp} = \Delta P_{tp,F} + \Delta P_{tp,G} + \Delta P_{tp,A}. \quad (1)$$

For flow boiling, $\Delta P_{tp,A}$ is the result of steam-wise acceleration along the channel and $\Delta P_{tp,A} > 0$. However, in condensing flows, the flow decelerates along the channel and $\Delta P_{tp,A} < 0$. This means

Table 3
Two-phase frictional pressure drop data for both adiabatic and condensing mini/micro-channel flows included in the consolidated database.

Author(s)	Channelgeometry*	Channel material	D_h [mm]	Fluid (s)	G [kg/m^{2}s]	Test mode	Data points
Hinde et al. [17]	C single, H	Copper	4.57	R134a, R12	149–298	Condensation Δx = 0.1–0.35	45
Wambsganss et al. [18]	R single, H	Plexiglas	5.44	Air–water	50–500	Adiabatic	112
Fujita et al. [19]	R single, H	Acrylic, nickel	0.39, 2.14, 3.33	N_2–water, N_2–ethanol	32–815	Adiabatic	167
Hirofumi and Webb [20]	C/R multi, H	Aluminum	0.96–2.13	R134a	194–1404	Adiabatic	58
Yang and Webb [21]	R multi, H	Aluminum	2.64	R12, R134a	400–1400	Adiabatic	64
Triplett et al. [22]	C/semi triangular single, H	Pyrex glass, acrylic	1.088, 1.097, 1.447	Air–water	23–6010	Adiabatic	192
Bao et al. [23]	C single, H	Copper	1.95	Air–water	110–435	Adiabatic	135
Coleman [24]	C single/multi, R multi, H	Aluminum	0.761–4.910	R134a	150–750	Adiabatic	245
Coleman [24]	C/R multi, H	Aluminum	0.424–1.524	R134a	150–750	Condensation Δx = 0.05–0.1	261
Wang et al. [25]	C single, H	Copper	3.0	R410A, R407C, R22	400	Adiabatic	45
Zhang and Webb [26]	C single/multi, H	Copper, aluminum	2.13, 3.25, 6.20	R134a, R22, R404A	400–1000	Adiabatic	72
Nino et al. [27]	R multi, H	Aluminum	1.02, 1.54	R410A, R134a	50–300	Adiabatic	364
Nino et al. [27]	R multi, H	Aluminum	1.02, 1.54	Air–water	55–220	Adiabatic	121
Adams et al. [28]	R multi, H	Aluminum	1.02, 1.54	CO2, ammonia, R245fa	50–440	Adiabatic	245
Monroe et al. [29]	R multi, H	Aluminum	1.66	R134a	49–402	Adiabatic	32
Pehlivan [30]	C single, H	Glass	0.8, 1.0, 3.0	Air–water	236–2252	Adiabatic	130
Jang and Hrnjak [31]	C single, H	Copper	6.10	CO_2	198–406	Adiabatic	54
Shin [32]	C/R single, H	Copper	0.493–1.067	R134a	100–600	Condensation small Δx	247
Tu and Hrnjak [33]	R single, H	PVC	0.0695–0.3047	R134a	102–785	Adiabatic	264
Cavallini et al. [34]	R multi, H	Aluminum	1.4	R410A, R134a, R236ea	200–1400	Adiabatic	51
Chen et al. [35]	C single, H	Copper	3.25	R410A	300–600	Adiabatic	26
Mitra [36]	C single, H	Copper	6.22	R410A	400–800	Condensation Δx = 0.21 (avg)	118
Andresen [37]	C single/multi, H	Aluminum, copper	0.76, 1.52, 3.05	R410A	200–800	Condensation Δx = 0.32 (avg)	291
English and Kandlikar [38]	R single, H	Lexan	1.018	Air–water	4–32	Adiabatic	40
Hwang and Kim [39]	C single, H	Stainless steel	0.244, 0.430, 0.792	R134a	140–950	Adiabatic	77
Yun et al. [40]	R multi, H	Stainless steel	1.437	R410A	200–400	Adiabatic	19
Field and Hrnjak [41]	R single, H	Aluminum	0.148	R134a, R410A, propane, ammonia	290–590	Adiabatic	67
Park and Hrnjak [42]	C single/multi, H	Aluminum, copper	0.89, 3.5, 6.1	CO2, R410A, R22	100–600	Adiabatic	146
Revellin and Thome [43]	C single, H	Glass	0.517	R134a, R245fa	309–1926	Adiabatic	1331
Yue et al. [44]	R single, H	PMMA	0.667	CO_2–water	91–1020	Adiabatic	105
Quan et al. [45]	trapezoidal multi, H	Silicon wafer, glass cover	0.109, 0.142, 0.151	Water	90–288	Condensation small Δx	65
Dutkowski [46]	C single, H	Stainless steel	0.64–2.30	Air–water	139–8528	Adiabatic	465
Marak [47]	C single, VU	Stainless steel	1.0	Methane	162–701	Condensation Δx = 0.04 (avg)	135
Park and Hrnjak [48]	C multi, H	Aluminum	0.89	CO2	200–800	Adiabatic	52
Huang et al. [49]	C single, H	Copper	1.6, 4.18	R410A	200–600	Condensation Δx = 0.2	35
Choi et al. [50]	R single, H	Glass	0.143, 0.322, 0.490	N_2–water	65–1080	Adiabatic	920
Ducoulombier et al. [51]	C single, H	Stainless steel	0.529	CO_2	200–1400	Adiabatic	292
Tibirica and Ribatski [52]	C single, H	Stainless steel	2.32	R245fa	100–500	Adiabatic	27
Total							7115

* C: circular, R: rectangular, H: horizontal, VU: vertical upward.

deceleration provides the benefit of decreasing the two-phase pressure drop. The accelerational pressure gradient can be expressed as

$$-\left(\frac{dP}{dz}\right)_A = G^2 \frac{d}{dz}\left[\frac{\upsilon_g x^2}{\alpha} + \frac{\upsilon_f (1-x)^2}{(1-\alpha)}\right] \tag{2}$$

where the void fraction, α, can be expressed in terms of flow quality, x, using Zivi's correlation [84],

$$\alpha = \left[1 + \left(\frac{1-x}{x}\right)\left(\frac{\rho_g}{\rho_f}\right)^{2/3}\right]^{-1} \tag{3}$$

For the homogeneous equilibrium model, the void fraction is related to flow quality by the relation

$$\alpha = \left[1 + \left(\frac{1-x}{x}\right)\left(\frac{\rho_g}{\rho_f}\right)\right]^{-1} \tag{4}$$

The gravitational pressure gradient is expressed as

$$-\left(\frac{dp}{dz}\right)_G = \left[\alpha\rho_g + (1-\alpha)\rho_f\right] g \sin\phi \tag{5}$$

where ϕ is the channel's inclination angle; $-(dp/dz)_G = 0$ for horizontal flows. Gravitational effects are negligible for mini/micro-channels compared to macro-channels, given the large shear stresses encountered in the former.

The two-phase frictional pressure drop, $\Delta P_{tp,F}$, is the result of wall frictional forces exerted upon the flow. The homogeneous equilibrium model treats the two-phase mixture as a pseudo fluid possessing properties that are dictated by local flow quality. In the homogeneous equilibrium model, the two-phase frictional pressure gradient can be determined from [85]

$$-\left(\frac{dP}{dz}\right)_F = \frac{2f_{tp}\bar{\rho}u^2}{D_h} = \frac{2f_{tp}\upsilon_f G^2}{D_h}\left(1 + x\frac{\upsilon_{fg}}{\upsilon_f}\right) \tag{6}$$

where

$$f_{tp} = 16\,Re_{tp}^{-1} \quad \text{for} \quad Re_{tp} < 2000, \tag{7a}$$

$$f_{tp} = 0.079\,Re_{tp}^{-0.25} \quad \text{for} \quad 2000 \leqslant Re_{tp} < 20,000, \tag{7b}$$

and

$$f_{tp} = 0.046\,Re_{tp}^{-0.2} \quad \text{for} \quad Re_{tp} \geqslant 20,000. \tag{7c}$$

Table 1 provides several two-phase mixture viscosity models that are used to calculate the two-phase Reynolds number, Re_{tp}.

Table 2 provides a summary of select two-phase frictional pressure drop correlations that have been recommended for macro-channels [60–63] and mini/micro-channels [21,39,64–70]. These include a mix of correlations for adiabatic and condensing flows. As discussed earlier, the two-phase frictional pressure drop correlations for flow boiling are excluded due to fundamental differences in droplet entrainment between condensing and adiabatic flows on one hand, and boiling flows on the other. Most of the correlations in Table 2 are based on the semi-empirical separated flow model (mostly Lockhart–Martinelli type [60]), where the two-phase frictional pressure gradient is expressed as the product of the frictional pressure gradient for each phase and a corresponding two-phase pressure drop multiplier

$$\left(\frac{dP}{dz}\right)_F = \left(\frac{dP}{dz}\right)_f \phi_f^2 = \left(\frac{dP}{dz}\right)_g \phi_g^2 \tag{8}$$

where the frictional pressure drop for each phase is based on the actual flow rate for the same phase,

$$-\left(\frac{dP}{dz}\right)_f = \frac{2f_f \upsilon_f G^2 (1-x)^2}{D_h} \tag{9a}$$

$$-\left(\frac{dP}{dz}\right)_g = \frac{2f_g \upsilon_g G^2 x^2}{D_h} \tag{9b}$$

In Eqs. (9a) and (9b), the Reynolds number and friction factor for each phase are also based on the actual flow rate for the same phase.

$$Re_f = \frac{G(1-x)D_h}{\mu_f} \quad \text{for liquid,} \tag{10a}$$

$$Re_g = \frac{GxD_h}{\mu_g} \quad \text{for vapor,} \tag{10b}$$

$$f_k = 16\,Re_k^{-1} \quad \text{for} \quad \mathrm{Re}_k < 2000 \tag{11a}$$

$$f_k = 0.079\,Re_k^{-0.25} \quad \text{for} \quad 2000 \leqslant \mathrm{Re}_k < 20,000 \tag{11b}$$

and

$$f_k = 0.046 \quad \mathrm{Re}_k^{-0.2} \quad \text{for} \quad \mathrm{Re}_k \geqslant 20,000 \tag{11c}$$

where the subscript k denotes f or g for liquid and vapor, respectively. For laminar flow in rectangular channel, the two-phase friction factor can be obtained from [86]

$$f_k \mathrm{Re}_k = 24\,(1 - 1.3553\,\beta + 1.9467\,\beta^2 - 1.7012\,\beta^3 + 0.9564\,\beta^4 - 0.2537\,\beta^5) \tag{12}$$

The correlations of Friedel [61] and Müller-Steinhagen and Heck [62] are widely adopted in the prediction of two-phase frictional pressure drop in macro-channels because they were derived from very large databases, 25,000 and 9300 pressure drop data points, respectively. The correlation of Mishima and Hibiki [64], which is based on adiabatic air–water flow in 1–4 mm diameter circular tubes, shows good predictions of the mini/micro-channel pressure drop data of Kim et al. [15], Pehlivan [30], Tu and Hrnjak [33], Yun et al. [40], Field and Hrnjak [41], and Quan et al. [45]. Notice that the correlations in Table

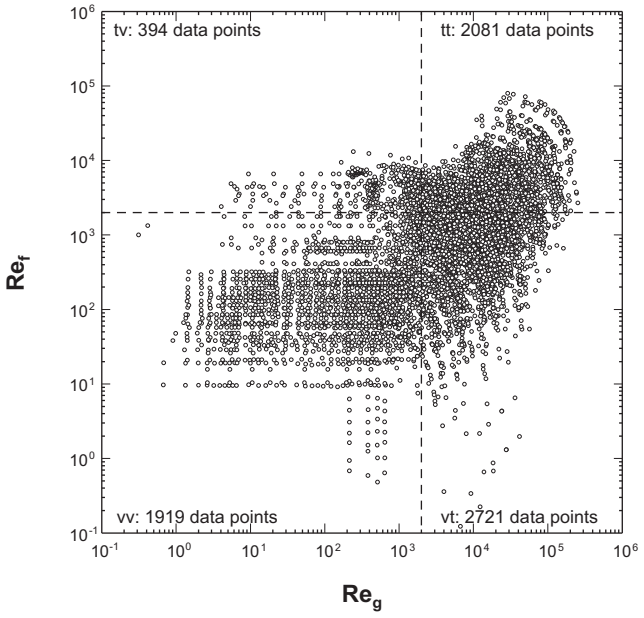

Fig. 2. Laminar/turbulent flow distribution of 7115 data points of consolidated database for two-phase frictional pressure drop in mini/micro-channels based on superficial liquid and vapor Reynolds numbers.

2 are valid only for the working fluids and ranges of operating conditions of the databases they are based upon.

Additionally, some correlations are recommended for specific laminar or turbulent flow states. For example, the correlations of Yang and Webb [21] and Yan and Lin [65], which are based on the equivalent Reynolds number Re_{eq} proposed by Akers et al. [54], are applicable only to turbulent flows ($Re_{fo} > 2500$ for [21], and $Re_{eq} > 2000$ for [65]). The correlation of Hwang and Kim [39] is based on pressure drop data for microtubes with diameters of 0.244, 0.430, and 0.792 mm corresponding to $Re_{fo} < 2000$. The correlation of Zhang et al. [70], which is a modified form of Mishima and Hibiki's [64], is not recommended for turbulent liquid–turbulent vapor flow.

Notice that the correlations in Table 2 are used to determine the two-phase frictional pressure gradient. The two-phase pressure drop can be determined by integrating Eqs. (2), (5), (6), and (8) numerically along the streamwise direction,

$$\Delta P_{tp} = \int_0^{L_{tp}} \left[-\left(\frac{dP}{dz}\right)_F - \left(\frac{dP}{dz}\right)_G - \left(\frac{dP}{dz}\right)_A \right] dz \tag{13}$$

3. New consolidated mini/micro-channel database

In the present study, a total of 7115 frictional pressure drop data points for both adiabatic and condensing flows in mini/micro-channels were amassed from 36 sources [17–52]. This database includes 2387 adiabatic gas–liquid data points from 10 sources, 3531 adiabatic liquid–vapor data points from 20 sources, and 1197 condensation data points from 8 sources.

Table 3 provides detailed information on individual databases incorporated into the consolidated database in chronological order along with the number of data points actually adopted. Some of the data are purposely excluded because they do not contribute to the development of a generalized pressure drop predictive method. For example, only pure liquid data from the databases of Hinde et al. [17], Fujita et al. [19], English and Kandlikar [38], Field and Hrnjak [41], Marak [47], and Huang et al. [49] are included in Table 3; all binary mixture, oil mixture, or surfactant solution data are excluded. Also excluded are all enhanced tube (*e.g.,* micro-fin tube) data from the databases of Yang and Webb [21], Zhang and Webb [26], and Monroe et al. [29], as well as barrel and N-shaped channels from Coleman [24], and U-type wavy tube data from Chen et al. [35]. For the Jang and Hrnjak [31] database, only horizontal data are included in Table 3.

Since the effects of surface roughness are not considered in this study, most of the data in the consolidated database, especially those for turbulent flow, are for smooth tubes with a relative roughness range of 0.001–0.0001. To exclude rough surfaces, 56 out of 191 data points from Marak [47] are excluded because their

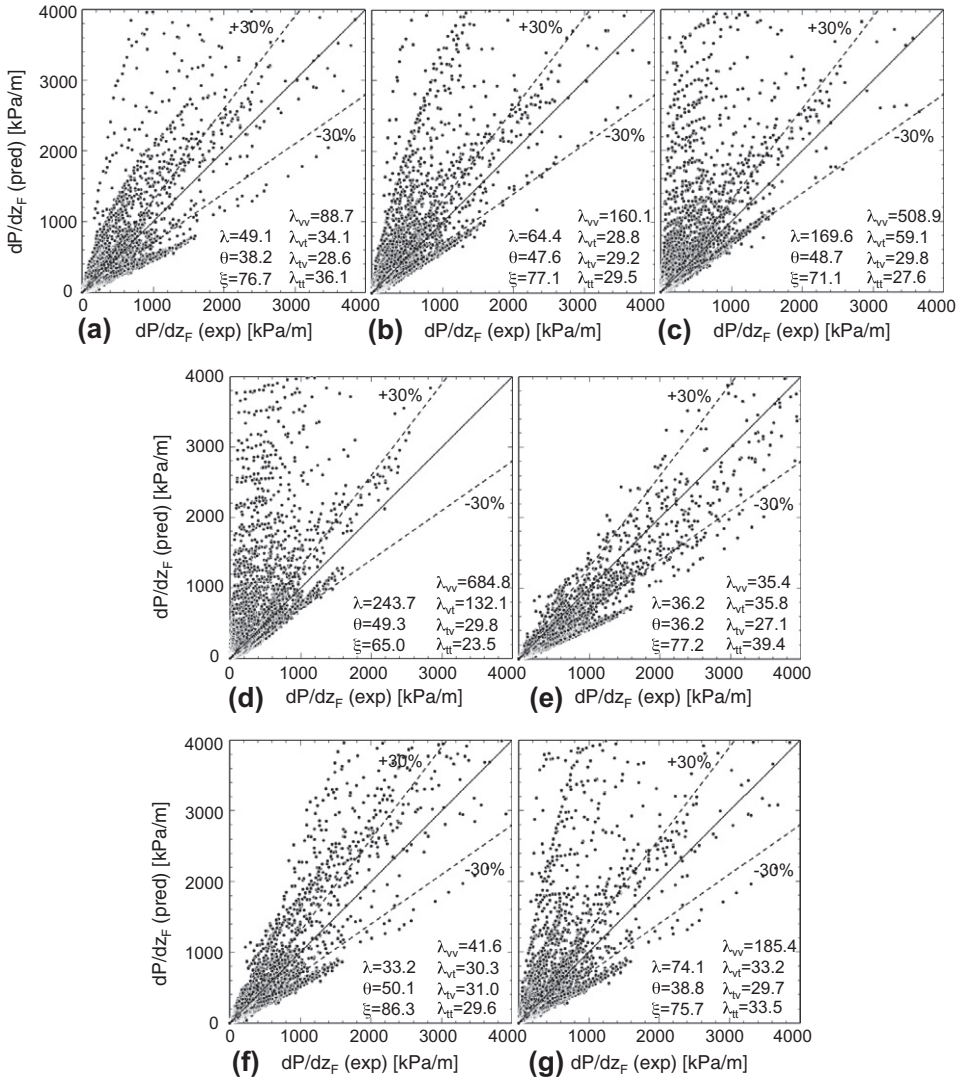

Fig. 3. Comparison of 7115 experimental data points with predictions of homogeneous models: (a) McAdams et al. [53], (b) Akers et al. [54], (c) Cicchitti et al. [55], (d) Owens [56], (e) Dukler et al. [57], (f) Beattie and Whalley [58], and (g) Lin et al. [59].

relative roughness exceeds 0.0024. The consolidated database also excludes hydrophobic (nonwetting) surfaces (*e.g.,* air–water flow on Teflon or Polytetrafluoroethylene (PTFE) surfaces) with a static contact angle larger than 90°.

A thorough inspection of the individual databases by the present authors identified duplicate data; which are also excluded from the consolidated database. Other data points are excluded because of their strong departure from the majority of comparable data. These include 77 of 562 data points from Nino et al. [27] corresponding to very low qualities or mass velocities, 568 data points for $D = 0.803$ mm from Revellin and Thome [43] (1331 data for $D = 0.517$ mm from the same source have been included). Also excluded for the same reason are the condensation data of Yan and Lin [65], Agarwal [87], and Bohdal et al. [88]. It should be noted that the database was closely inspected by relying on published data from original sources.

All condensation data included in Table 3 correspond to a relatively small quality decrement, Δx. Therefore, an average of the inlet and outlet qualities is used in the development of a pressure drop correlation based on the assumption of linear quality variation along the channel. Also, due to the small quality decrements, the contribution of the deceleration term to total pressure drop is found to be quite small for most of the data. For example, $\Delta P_{tp,A}/\Delta P_{tp}$ is about less than 2.0% for the Coleman data [24]. When calculating the deceleration term, Coleman [24], Mitra [36], Andresen [37], and Marak [47] used Baroczy's [89] void fraction relation, while Huang et al. [49] used Rouhani and Axelsson's [90] void fraction relation,

$$\alpha = \left[1 + \left(\frac{1-x}{x}\right)^{0.74}\left(\frac{\rho_g}{\rho_f}\right)^{0.65}\left(\frac{\mu_f}{\mu_g}\right)^{0.13}\right]^{-1} \tag{14}$$

and

$$\alpha = \frac{x}{\rho_g}\left[\{1+0.12(1-x)\}\left(\frac{x}{\rho_g}+\frac{1-x}{\rho_f}\right)+\frac{1.18(1-x)\{g\sigma(\rho_f-\rho_f)\}^{0.25}}{G\rho_f^{0.5}}\right]^{-1} \tag{15}$$

respectively. In case of a significant quality decrement, such as high-flux micro-channel condensing flows, deceleration contributes an appreciable fraction of total pressure drop due to the increasing amount of vapor being condensed. The effect of using different void fraction models to determine the accelerational pressure drop is examined later based on prior experimental FC72 condensation data by the present authors [15].

Unlike prior databases that have been used to correlate frictional pressure drop in mini/micro-channels, the present consolidated database includes a broad range of reduced pressures, from 0.0052 to 0.91. Included here are databases covering high reduced pressure values beyond 0.5 by Zhang and Webb [26] (P_R = 0.21–0.51), Adams et al. [28] (P_R = 0.07–0.69), and Ducoulombier et al. [51] (P_R = 0.36–0.54). Also included are two-phase frictional pressure drop data approaching critical pressure by Mitra [36] (P_R = 0.8–0.9), Andresen [37] (P_R = 0.8–0.9), and Marak [47] (P_R = 0.14–0.91).

In all, the new consolidated database includes 7115 frictional pressure drop data points with the following coverage:

- Working fluid: air/CO_2/N_2–water mixtures, N_2–ethanol mixture, R12, R22, R134a, R236ea, R245fa, R404A, R410A, R407C, propane, methane, ammonia, CO_2, and water
- Hydraulic diameter: $0.0695 < D_h < 6.22$ mm
- Mass velocity: $4.0 < G < 8528$ kg/m^2 s
- Liquid-only Reynolds number: $3.9 < \mathrm{Re}_{fo} = GD_h/\mu_f < 89798$
- Superficial liquid Reynolds number: $0 < \mathrm{Re}_f = G(1-x)D_h/\mu_f < 79202$
- Superficial vapor (or gas) Reynolds number: $0 < \mathrm{Re}_g = GxD_h/\mu_g < 253810$
- Flow quality: $0 < x < 1$
- Reduced pressure (for 4728 condensing and adiabatic liquid–vapor data): $0.0052 < P_R < 0.91$

Fig. 2 shows all 7115 data points in a plot of superficial liquid Reynolds number versus superficial gas Reynolds number. With a transition Reynolds number value of 2000, 1919 data points are laminar liquid–laminar vapor (vv), 2721 laminar liquid–turbulent vapor (vt), 394 turbulent liquid–laminar vapor (tv), and 2081 turbulent liquid–turbulent vapor (tt).

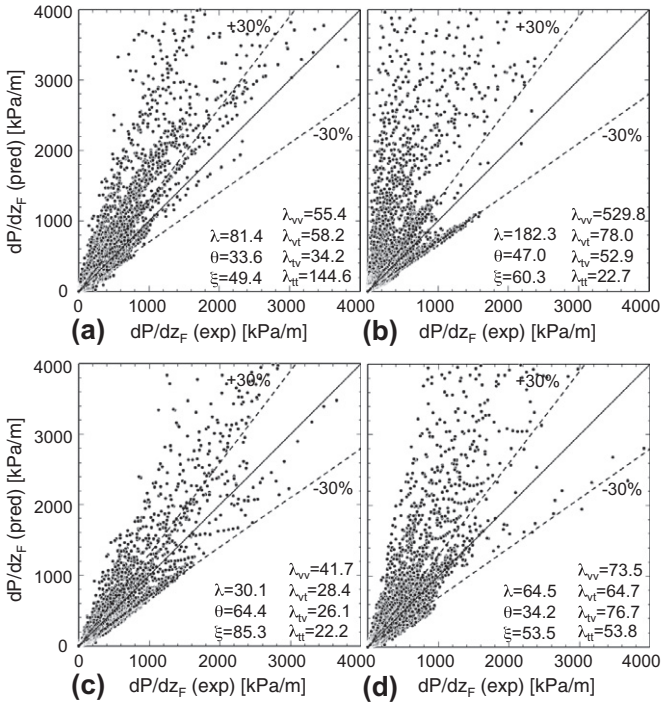

Fig. 4. Comparison of 7115 experimental data points with predictions of semi-empirical correlations recommended for macro-channels: (a) Lockhart and Martinelli [60], (b) Friedel [61], (c) Müller-Steinhagen and Heck [62], and (d) Wang et al. [63].

4. Evaluation of previous correlations

Figs. 3–5 compare the 7115 frictional pressure drop data points for both adiabatic and condensing mini/micro-channel flows with predictions of previous homogeneous equilibrium models [53–59], and semi-empirical correlations for both macro-channels [60–63] and mini/micro-channels [21,39,64–70], respectively. Thermophysical properties for liquid and vapor in Figs. 3–5 and all subsequent calculations are based on REFPROP 8.0 software from NIST [91].

The accuracy of individual models is evaluated by θ and ξ which are the percentages of data points predicted within ±30% and ±50%, respectively, and mean absolute error, defined as

$$\mathrm{MAE} = \frac{1}{N}\sum\frac{|dP/dz_{\mathrm{F,pred}} - dP/dz_{\mathrm{Fexp}}|}{dP/dz_{\mathrm{F},exp}} \times 100\% \tag{16}$$

The percentage value of MAE is indicated in Figs. 3–5 as λ, with λ_{vv}, λ_{vt}, λ_{tv} and λ_{tt} indicating MAE percentage values for laminar liquid–laminar vapor (vv), laminar liquid–turbulent vapor (vt), turbulent liquid–laminar vapor (tv), and turbulent liquid–turbulent vapor (tt), respectively.

As shown in Fig. 3, most of the homogeneous equilibrium models overpredict the pressure drop data in the laminar–laminar (vv) and laminar–turbulent (vt) regimes. Most noticeable are the models of McAdams et al. [53], Akers et al. [54], and Lin et al. [59] highly overpredicting the data in the laminar–laminar (vv) regime, and those of Cicchitti et al. [55] and Owens [56] highly overpredicting the data in both the laminar–laminar (vv) and laminar–turbulent (vt) regimes. Among all homogeneous equilibrium models, only those of Dukler et al. [57] and Beattie and Whalley [58] show relatively fair predictions for all flow regimes, with MAE values of 36.2%, and 33.2%, respectively.

Fig. 4 shows the frictional pressure drop correlations recommended for macro-channels overpredict most of the consolidated frictional pressure gradient database. The correlations by Lockhart and Martinelli [60] and Friedel [61] show the greatest departure, with MAE values of 81.4% and 182.3%, respectively. The Wang et al. correlation [63] shows large scatter for all flow regimes. Most notably, the correlation of Müller-Steinhagen and Heck [62], which is based on macro-channel data with diameters larger than 4 mm, provides the best predictions among all previous models and correlations in Figs. 3–5, evidenced by a MAE of 30.1%, although its predictions are less favorable in the laminar–laminar (vv) regime.

As shown in Fig. 5, frictional pressure drop correlations intended for mini/micro-channels provide fair to poor predictions of the consolidated database. Notice that for the correlations of Yang and Webb [21], Yan and Lin [65], Hwang and Kim [39], Li and Wu [69], and Zhang et al. [70], only the pressure drop data corresponding to their validity range are considered. The correlations of Yan and Lin [65] and Lee and Lee [66] show significant scatter, with MAE values of 178.0%, and 101.6%, respectively. The correlations of Mishima and Hibiki [64] and Sun and Mishima [68] show poor predictions in the turbulent–turbulent (tt), and laminar–laminar (vv) regimes, respectively. While Zhang et al. correlation, which is a modified correlation of Mishima and Hibiki, provides a better overall MAE than that Mishima and Hibiki's, its predictions are worse for three flow regimes (vv, vt, and tv). Among all previous mini/micro-channel correlations, Yang and Webb's shows the best predictions when applied to data with $Re_{fo} > 2500$ as recommended by the original authors.

5. New predictive two-phase pressure drop method

The new universal approach to predicting two-phase frictional pressure drop for adiabatic and condensing mini/micro-channel flows utilizes the original formulation of Lockhart and Martinelli

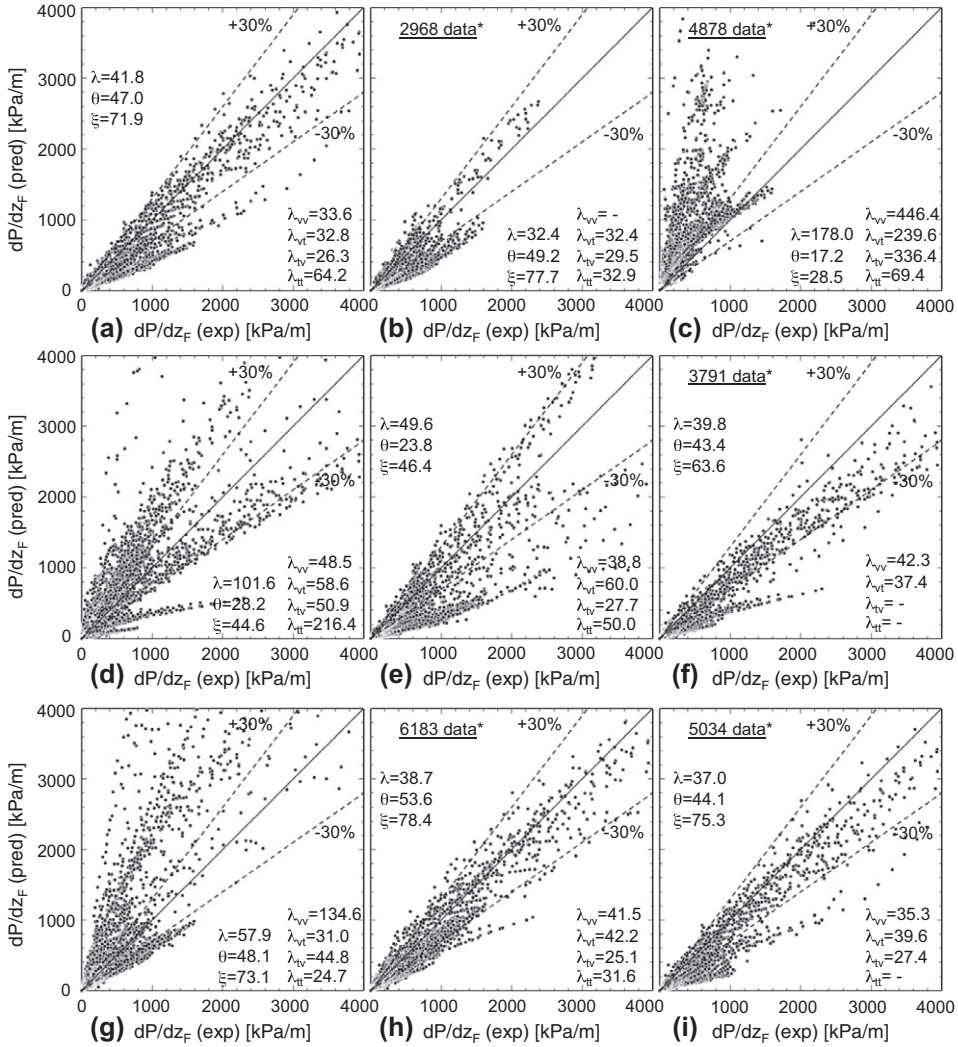

Fig. 5. Comparison of 7115 experimental data points with predictions of semi-empirical correlations recommended for mini/micro-channels: (a) Mishima and Hibiki [64], (b) Yang and Webb [21], (c) Yan and Lin [65], (d) Lee and Lee [66], (e) Chen et al. [67], (f) Hwang and Kim [39], (g) Sun and Mishima [68], (h) Li and Wu [69], and (i) Zhang et al. [70]. Data indicated (∗) correspond to Refo > 2500 for Yang and Webb [21] , Reeq > 2000 for Yan and Lin [65], Refo < 2000 for Hwang and Kim [39], Bo < 11 for Li and Wu [69], and data excluding turbulent liquid–turbulent vapor (tt) for Zhang et al. [70].

[60], modified with new dimensionless groups that account for small channel hydraulic diameter, and validated against the new consolidated database. In particular, the constant C in the Lockhart–Martinelli parameter is replaced by a function of appropriate dimensionless groups that capture the influence of small channels.

Table 4 summarizes the dimensionless groups that have been used in the past to predict two-phase frictional pressure drop. These groups are mostly different combinations of inertia, viscous force, surface tension force and body (or buoyancy) force. What distinguishes mini/micro-channels from macro-channels is the significance of surface tension and viscosity effects and negligible body force effects for the former as discussed by Qu and Mudawar [16] and Kim and Mudawar [79]. Notice that the Froude, Bond, Confinement, and Galileo numbers in Table 4 are measures of body force effects and as such, not appropriate for mini/micro-channel predictions. To account for the net influence of interactions among inertia, viscous force, and surface tension, choices of dimensionless parameters include combinations of Reynolds, Weber, Capillary, and Suratman numbers. Density ratio is also considered to both cope with different working fluids, such as air/CO_2/N_2-water mixtures, refrigerants, propane, methane, ammonia, CO_2, and water, and broad variations in reduced pressure.

Using the entire consolidated database, C functions of various combinations of Reynolds, Weber, Capillary, and Suratman numbers and density ratio were attempted for each of the four combinations of flow regimes (tt, tv, vt, and vv). Table 5 provides a summary of the functions yielding the least MAE versus the database. A relatively simple function of liquid-only Reynolds number, Re_{fo}, vapor-only (or gas-only) Suratman number, Su_{go}, and density ratio, ρ_f/ρ_g, provides good predictions for each of the four flow regimes. Fig. 6 shows the new two-phase frictional pressure drop correlation, which is summarized in Table 5, predicts the entire 7115 experimental mini/micro-channel database quite accurately, with MAE values of 26.3%, 22.4%, 26.8%, and 21.1% for the laminar–laminar (vv), laminar–turbulent (vt), turbulent–laminar (tv), turbulent–turbulent (tt) flow regimes, respectively.

Notice that for the turbulent–laminar (tv) flow regime, relatively good overall predictions over the entire database are achieved using the models or correlations by Dukler et al. [57], Müller-Steinhagen

Table 5
New pressure drop correlation for mini/micro-channels in both single- and multi-channel configurations.

$$\left(\frac{dP}{dz}\right)_F = \left(\frac{dP}{dz}\right)_f \phi_f^2$$

where

$$\phi_f^2 = 1 + \frac{C}{X} + \frac{1}{X^2},\ X^2 = \frac{(dP/dz)_f}{(dP/dz)_g}$$

$$-\left(\frac{dP}{dz}\right)_f = \frac{2f_f \upsilon_f G^2 (1-x)^2}{D_h},\ -\left(\frac{dP}{dz}\right)_g = \frac{2f_g \upsilon_g G^2 x^2}{D_h}$$

$f_k = 16\,\mathrm{Re}_k^{-1}$ for $\mathrm{Re}_k < 2000$

$f_k = 0.079\,\mathrm{Re}_k^{-0.25}$ for $2000 \leqslant \mathrm{Re}_k < 20{,}000$

$f_k = 0.046\,\mathrm{Re}_k^{-0.2}$ for $\mathrm{Re}_k \geqslant 20{,}000$

for laminar flow in rectangular channel,

$$f_k Re_k = 24\,(1 - 1.3553\,\beta + 1.9467\,\beta^2 - 1.7012\,\beta^3 + 0.9564\,\beta^4 - 0.2537\,\beta^5)$$

where subscript k denotes f or g for liquid and vapor phases, respectively,

$$Re_f = \frac{G(1-x)D_h}{\mu_f},\ Re_g = \frac{GxD_h}{\mu_g},\ Re_{fo} = \frac{GD_h}{\mu_f},\ Su_{go} = \frac{\rho_g \sigma D_h}{\mu_g^2}$$

Liquid	Vapor (gas)	C
Turbulent	Turbulent	$0.39 Re_{fo}^{0.03} Su_{go}^{0.10} \left(\frac{\rho_f}{\rho_g}\right)^{0.35}$
Turbulent	Laminar	$8.7 \times 10^{-4} Re_{fo}^{0.17} Su_{go}^{0.50} \left(\frac{\rho_f}{\rho_g}\right)^{0.14}$
Laminar	Turbulent	$0.0015 Re_{fo}^{0.59} Su_{go}^{0.19} \left(\frac{\rho_f}{\rho_g}\right)^{0.36}$
Laminar	Laminar	$3.5 \times 10^{-5} Re_{fo}^{0.44} Su_{go}^{0.50} \left(\frac{\rho_f}{\rho_g}\right)^{0.48}$

Table 4
Dimensionless groups that have been employed in the prediction of two-phase pressure gradient.

Parameter	Definition	Interpretation
Liquid- or gas-only Reynolds number	$Re_{fo} = \frac{GD_h}{\mu_f}$ $Re_{go} = \frac{GD_h}{\mu_g}$	$\frac{\text{Inertia}}{\text{Viscous force}}$ based on total flow rate
Superficial liquid or gas Reynolds number	$Re_f = \frac{G(1-x)D_h}{\mu_f}$ $Re_g = \frac{GxD_h}{\mu_g}$	$\frac{\text{Inertia}}{\text{Viscous force}}$ based on actual flow rate for each phase
Density ratio	$\frac{\rho_f}{\rho_g}$	$\frac{\text{Liquid density}}{\text{Vapor density}}$
Weber number	$We = \frac{G^2 D_h}{\rho_f \sigma}$	$\frac{\text{Inertia}}{\text{Surface tension force}}$
Capillary number	$Ca = \frac{\mu_f G}{\rho_f \sigma}\ (= \frac{We}{Re_{fo}})$	$\frac{\text{Viscous force}}{\text{Surface tension force}}$
Liquid- or gas-only Suratman number	$Su_{fo} = \frac{\rho_f \sigma D_h}{\mu_f^2}\ (= \frac{Re_{fo}^2}{We})$ $Su_{go} = \frac{\rho_g \sigma D_h}{\mu_g^2}\ (= \frac{Re_{go}^2}{We})$	–
Froude number	$Fr = \frac{G^2}{g D_h \rho_f^2}$	$\frac{\text{Inertia}}{\text{Body force}}$
Bond number	$Bo = \frac{g(\rho_f - \rho_g) D_h^2}{\sigma}$	$\frac{\text{Bouyancy force}}{\text{Surface tension force}}$
Confinement number	$N_{conf} = \sqrt{\frac{\sigma}{g(\rho_f - \rho_g) D_h^2}}\ \left(= \sqrt{\frac{1}{Bo}}\right)$	$\sqrt{\frac{\text{Surface tension force}}{\text{Body force}}}$
Galileo number	$Ga = \frac{\rho_f g (\rho_f - \rho_g) D_h^3}{\mu_f^2}$	–
Lockhart–Martinelli parameter	$X_{vv} = \left(\frac{\mu_f}{\mu_g}\right)^{0.5} \left(\frac{1-x}{x}\right)^{0.5} \left(\frac{\rho_g}{\rho_f}\right)^{0.5}$ $X_{vt} = \left(\frac{f_f}{f_g}\right)^{0.5} \left(\frac{1-x}{x}\right)^{1.0} \left(\frac{\rho_g}{\rho_f}\right)^{0.5}$ $X_{tv} = \left(\frac{f_f}{f_g}\right)^{0.5} \left(\frac{1-x}{x}\right)^{1.0} \left(\frac{\rho_g}{\rho_f}\right)^{0.5}$ $X_{tt} = \left(\frac{\mu_f}{\mu_g}\right)^{0.1} \left(\frac{1-x}{x}\right)^{0.9} \left(\frac{\rho_g}{\rho_f}\right)^{0.5}$	Based on laminar liquid–laminar turbulent (vv), laminar liquid–turbulent vapor (vt), turbulent liquid–laminar vapor (tv), turbulent liquid–turbulent vapor (tt), where f_f and f_g are given by Eqs. (11a), (11b), (11c)

and Heck [62], Mishima and Hibiki [64], Chen et al. [67], Li and Wu [69], and Zhang et al. [70], with MAE values of 27.1%, 26.1%, 26.3%, 27.7%, 25.1%, and 27.4%, respectively. Successful predictions of these model and correlations for this specific regime (tv) can be attributed largely to the fact that most data points corresponding to this regime (214 of 394 points) come from a single source, Dutkowski's [46]. For most of the other individual databases, the new correlation shows the best predictions in the turbulent–laminar (tv) flow regime compared to afore-mentioned models and correlations. A key attribute of the present method is its ability to predict data quite accurately for all individual databases.

Achieving low overall values for MAE is by no means the only definitive means for ascertaining the effectiveness of the new predictive approach. It is also vitally important that the correlation be evenly successful at predicting data over relatively broad variations of individual flow parameters. As discussed in [82,83], this notion is often overlooked in the literature when assessing the effectiveness of new correlations.

To explore this issue, it is also important to examine the distribution of number of available data points relative to the individual parameters. Fig. 7 shows, for each parameter, both a lower bar chart distribution of number of data points, and corresponding upper bar chart distribution of MAE in the predictions of the new frictional pressure drop correlation. The distribution of the entire 7115 point database is examined in this manner relative to working fluid, hydraulic diameter, D_h, mass velocity, G, liquid-only Reynolds number, Re_{fo}, quality, x, and reduced pressure, P_R. The database consists of 2387 adiabatic liquid–gas data points from 10 sources, 3531 adiabatic liquid–vapor data points from 20 sources, and 1197 condensation data points from 8 sources, and includes 17 different working fluids. Overall, the new correlation shows excellent predictions for most parameter bins with MAE values around 20%, indicating that the accuracy is not compromised over the ranges of individual parameters.

Another measure of the predictive accuracy of the new correlation is the ability to provide evenly good predictions for individual databases comprising the consolidated database. Table 6 compares individual mini/micro-channel databases from 36 sources with predictions of the present correlation as well as select previous models and correlations that have shown relatively superior predictive capability as discussed earlier. Akers et al. [54] model shows good prediction of some of the turbulent data such as those of Hirofumi and Webb [20], Cavallini et al. [34], and Park and Hrnjak [48]. The model by Dukler et al. [57] shows good prediction of some of the data for adiabatic liquid–gas flow such as those of Fujita et al. [19], Nino et al. [27], Adams et al. [28], and Dutkowski [46]. Although the correlation of Müller-Steinhagen and Heck [62] provided the best overall predictions among the previous models and correlations, it shows poor predictions against most adiabatic liquid–gas flow databases. Table 6 shows the new correlation

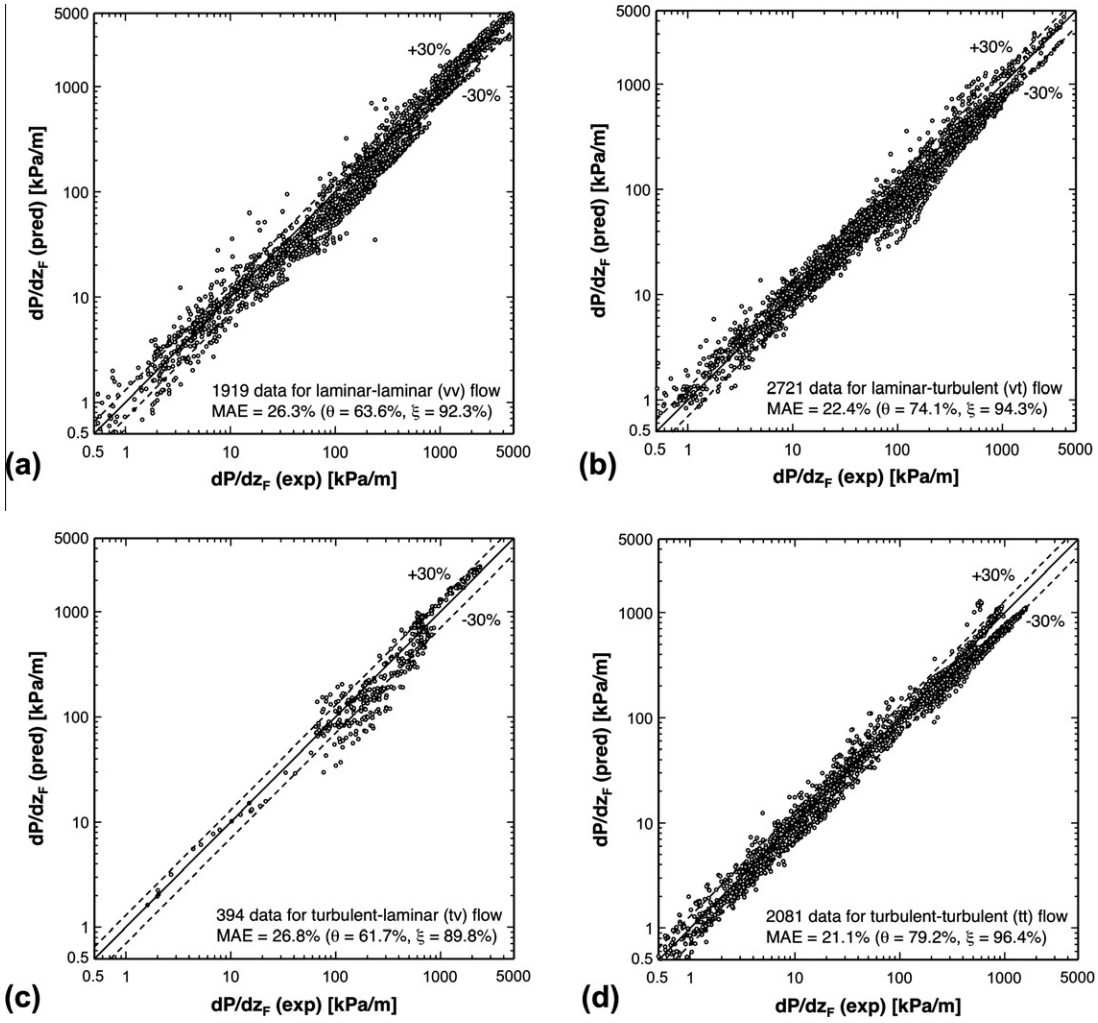

Fig. 6. Comparison of predictions of new frictional pressure drop correlation with 7115 mini/micro-channel data points for: (a) laminar–laminar (vv), (b) laminarturbulent (vt), (c) turbulent–laminar (tv), and (d) turbulent–turbulent (tt) flow regimes.

provides good predictions for all individual databases, with 19 databases predicted more accurately than any of the previous models or correlations, and the best overall MAE of 23.3%.

Another measure of the predictive capability of the new correlation is to evaluate its predictions versus three separate subsets of the consolidated database: adiabatic liquid–gas flow, adiabatic liquid–vapor flow, and condensing flow. Table 7 compares the predictions of the new correlation to those of the previous models and correlations for each of the three subsets. Most of the viscosity models used in conjunction with the homogeneous equilibrium model, excepting those of Dukler et al. [57] and Beattie and Whalley [58], show poor predictions for the adiabatic liquid–gas flow data. The correlations of Mishima and Hibiki [64] and Lee and Lee [66], which are based on adiabatic air–water flow, provide poor predictions of both adiabatic liquid–vapor and condensation data. The correlation of Sun and Mishima [68] provides poor predictions overall, especially for adiabatic liquid–gas flow, with a MAE value of 108.1%. Overall, relatively good predictions are shown by the viscosity model of Dukler et al. and correlation by Mishima and Hibiki for adiabatic liquid–gas data (MAE values of 33.7% and 34.1%, respectively), and Akers et al. [54], Beattie and Whalley [58] and Müller-Steinhagen and Heck [62] for adiabatic liquid–vapor data (MAE values of 32.4%, 33.2%, and 26.0%, respectively), Akers et al., Beattie and Whalley [58] Müller-Steinhagen and Heck [62], Yang and Webb [21], and Sun and Mishima [68] for condensation data (MAE values of 27.2%, 27.6%, 23.6%, 23.6%, and 23.0%, respectively). However, these previous models and correlations fail to provide evenly good predictions for all three data subsets. The new correlation shows the best predictions for all three subsets of adiabatic liquid–gas flow, adiabatic liquid–vapor flow, and condensing flow, with MAE values of 25.7%, 23.7%, and 17.5%, respectively. The results for the new correlation are also illustrated graphically in Fig. 8.

Fig. 9 shows predictions of the new correlation compared to two subsets of the entire consolidated database: multi-channel flow and flow in single channels. For the 1661 multi-channel data subset, the MAE is 18.7%, with 82.2% and 94.9% of the data falling within ±30% and ±50% error bands, respectively. The MAE for the 5454 single-channel data subset is 24.7%, with 69.0% and 93.9% of the data falling within ±30% and ±50% error bands, respectively. The overall MAE based on the entire 7115 point database is 23.3%, with 72.1% and 94.1% of the data falling within ±30% and ±50% error bands, respectively.

As indicated earlier, the accelerational pressure gradient is negligible for most condensation databases included in Table 3. One exception is situations involving high-flux condensation and appreciable axial variations in flow quality between the micro-channel inlet and outlet. This is the case with a recent database obtained by the authors [15]. This database involved condensation of FC72 along parallel 29.9-cm long micro-channels with a hydraulic diameter of 1 mm, that were machined into the top surface of a solid copper plate, which showed significant quality change between the micro-channel inlet and outlet, from 0.4 to 1.0. To isolate the frictional pressure gradient from the measurements, the decelerational pressure gradient is determined using Eq. (2) and Zivi's [84]

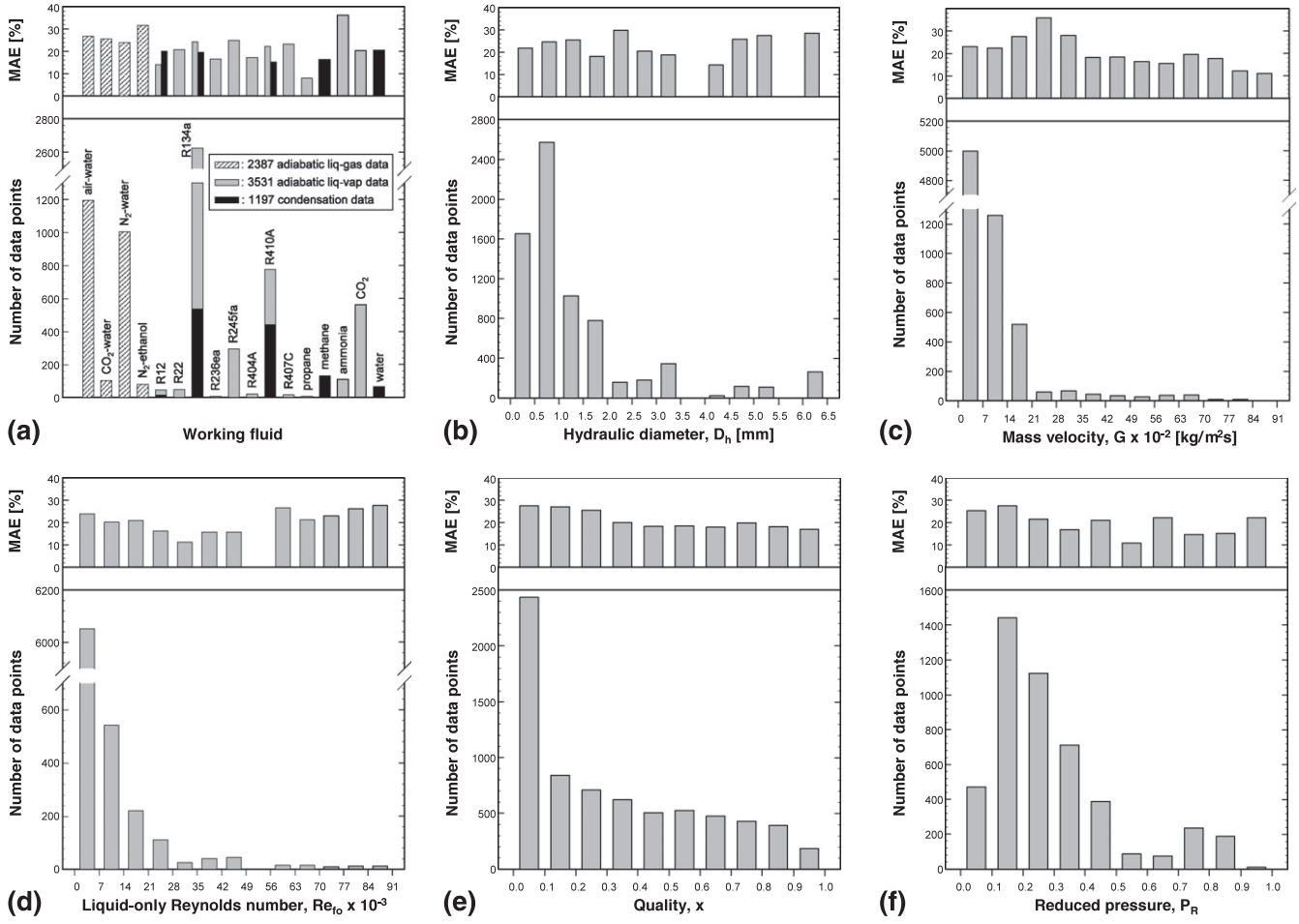

Fig. 7. Distributions of number of data points and MAE in predictions of new correlation method for entire 7115 point database relative to: (a) working fluid, (b) hydraulic diameter, (c) mass velocity, (d) liquid-only Reynolds number, (e) quality, and (f) reduced pressure (for 4728 condensing and adiabatic liquid vapor data).

void fraction relation, Eq. (3). Fig. 10(a) compares the experimental frictional pressure gradient with predictions of both the new correlation and two correlations that showed the best predictions among the previous models and correlations. The new correlation shows the best overall predictions, with a MAE of 25.4%, compared to 54.9% for Müller-Steinhagen and Heck [62], and 27.2% for Mishima and Hibiki [64].

Fig. 10(b) compares the same FC72 data [15] with the predictions of the new frictional pressure drop correlation, but with the accelerational pressure gradient (negative for condensing flows) determined using different void fraction models. Despite the appreciable axial changes in quality between the channel inlet and outlet, Fig. 10(b) shows that using the different void fraction relations of Zivi [84], Baroczy [89], and Rouhani and Axelsson [90] provides fairly similar results, evidenced by MAE values of 25.4%, 25.3%, and 25.5%, respectively. However, the void fraction relation derived from the homogeneous equilibrium model, Eq. (4), slightly overpredicts the experimental data compared to the other void fraction relations, with a MAE of 29.1%, especially for mass velocities in the range of 248 to 367 kg/m^2 s. It can therefore be concluded that, in situations involving appreciable quality changes, the choice of void fraction relation in determining accelerational pressure gradient is relatively insignificant compared to the choice of frictional gradient correlation.

Despite the success of the present correlation method in predicting the two-phase frictional gradient for mini/micro-channels,

Table 6
Comparison of individual mini/micro-channel frictional pressure drop databases with predictions of present correlation and select previous models and correlations.

Database author(s)	Fluid(s)	Test mode	Mean absolute error (%)					
			Akers et al. [54]	Dukler et al. [57]	Beattie and Whalley [58]	Müller-Steinhagen and Heck [62]	Mishima and Hibiki [64]	New correlation
Hinde et al. [17]	R134a, R12	Condensation	44.6	54.3	47.2	35.4	62.7	31.3
Wambsganss et al. [18]	Air–water	Adiabatic	44.7	38.5	39.5	48.5	57.7	27.4
Fujita et al. [19]	N_2–water, N_2–ethanol	Adiabatic	182.3	27.6	52.9	34.5	67.1	33.9
Hirofumi and Webb [20]	R134a	Adiabatic	13.8	23.9	18.1	21.2	55.1	25.3
Yang and Webb [21]	R12, R134a	Adiabatic	35.3	45.4	36.7	19.7	50.1	14.6
Triplett et al. [22]	Air–water	Adiabatic	80.0	32.7	24.2	36.6	37.0	21.8
Bao et al. [23]	Air–water	Adiabatic	39.3	42.8	21.3	27.1	25.3	19.5
Coleman [24]	R134a	Adiabatic	22.8	36.8	28.4	14.6	41.0	15.7
Coleman [24]	R134a	Condensation	17.3	31.1	21.0	18.8	19.3	14.0
Wang et al. [25]	R410A, R407C, R22	Adiabatic	43.0	54.2	47.8	26.2	27.3	25.0
Zhang and Webb [26]	R134a, R22, R404A	Adiabatic	18.7	32.2	23.9	11.7	80.4	16.3
Nino et al. [27]	R410A, R134a	adiabatic	18.8	32.4	24.8	21.4	22.6	14.8
Nino et al. [27]	Air–water	Adiabatic	67.9	21.4	22.5	73.0	44.1	22.6
Adams et al. [28]	CO2, ammonia, R245fa	Adiabatic	29.0	24.9	25.6	44.4	46.4	29.8
Monroe et al. [29]	R134a	Adiabatic	29.3	48.4	41.1	16.7	23.3	24.2
Pehlivan [30]	Air–water	Adiabatic	58.3	45.5	51.9	52.4	28.8	30.9
Jang and Hrnjak [31]	CO_2	Adiabatic	27.0	39.4	31.4	10.6	95.2	24.7
Shin [32]	R134a	Condensation	29.9	44.4	36.5	16.1	24.8	23.4
Tu and Hrnjak [33]	R134a	Adiabatic	78.9	23.2	46.7	29.9	21.3	18.2
Cavallini et al. [34]	R410A, R134a, R236ea	Adiabatic	23.7	31.8	30.9	33.4	52.2	32.9
Chen et al. [35]	R410A	Adiabatic	24.3	35.0	28.5	9.6	76.6	21.3
Mitra [36]	R410A	Condensation	39.5	44.0	37.5	26.3	148.2	23.0
Andresen [37]	R410A	Condensation	19.9	26.7	16.8	14.9	103.5	11.7
English and Kandlikar [38]	Air–water	Adiabatic	135.6	18.4	11.0	35.6	59.7	8.1
Hwang and Kim [39]	R134a	Adiabatic	40.1	32.1	38.1	51.5	25.0	31.4
Yun et al. [40]	R410A	Adiabatic	27.4	43.7	35.5	12.1	18.9	11.8
Field and Hrnjak [41]	R134a, R410A, propane, ammonia	Adiabatic	42.9	18.7	26.5	47.5	17.8	15.2
Park and Hrnjak [42]	CO2, R410A, R22	Adiabatic	31.7	41.2	36.2	25.9	58.2	31.0
Revellin and Thome [43]	R134a, R245fa	Adiabatic	33.1	47.1	36.9	27.6	49.8	29.1
Yue et al. [44]	CO_2–water	Adiabatic	115.0	54.6	25.7	25.8	33.0	25.6
Quan et al. [45]	Water	Condensation	39.1	27.3	26.1	115.3	16.7	20.5
Dutkowski [46]	Air–water	Adiabatic	45.5	29.5	32.7	32.1	34.1	32.1
Marak [47]	Methane	Condensation	28.6	37.7	30.7	17.6	37.8	16.2
Park and Hrnjak [48]	CO2	Adiabatic	13.1	17.0	13.1	29.2	23.1	33.7
Huang et al. [49]	R410A	Condensation	39.6	48.6	40.5	21.5	56.0	18.4
Choi et al. [50]	N_2–water	Adiabatic	218.3	33.4	40.7	40.6	24.3	22.9
Ducoulombier et al. [51]	CO_2	Adiabatic	24.9	37.2	29.2	15.3	25.4	14.3
Tibirica and Ribatski [52]	R245fa	Adiabatic	18.6	42.8	34.0	14.3	22.8	15.7
Total			64.4	36.2	33.2	30.1	41.8	23.3

Table 7
Assessment of present correlation and previous models and correlations with two-phase frictional pressure gradient databases for adiabatic liquid–gas flow, adiabatic liquid–vapor flow, and flow condensation (bracketed values stand for number of data used for evaluation).

Author(s)	Adiabatic liquid–gas (total 2387 data)			Adiabatic liquid–vapor (total 3531 data)			Condensation (total 1197 data)		
	λ(%)	θ (%)	ξ (%)	λ (%)	θ (%)	ξ (%)	λ (%)	θ (%)	ξ (%)
McAdams et al. [53]	75.0	44.8	61.7	35.2	35.8	83.2	38.4	32.3	87.6
Akers et al. [54]	130.5	37.4	49.6	32.4	50.9	89.6	27.2	57.9	95.2
Cicchitti et al. [55]	412.1	27.9	38.7	41.1	59.0	85.8	65.0	60.0	92.1
Owens [56]	571.3	25.9	36.8	71.6	59.2	76.3	98.1	66.6	87.9
Dukler et al. [57]	33.7	48.6	77.8	38.1	29.6	73.7	35.9	31.0	86.2
Beattie and Whalley [58]	36.1	58.2	78.5	33.2	43.7	88.9	27.6	53.0	94.2
Lin et al. [59]	150.4	35.9	50.5	34.1	40.7	88.2	40.2	38.8	89.4
Lockhart and Martinelli [60]	47.1	44.2	70.9	83.6	32.1	42.7	142.9	17.0	26.1
Friedel [61]	422.9	14.7	24.5	62.2	60.3	76.0	56.7	72.3	85.6
Muller-Steinhagen and Heck [62]	39.3	50.6	73.9	26.0	68.8	90.1	23.6	79.2	93.7
Wang et al. [63]	63.1	32.7	55.8	59.1	40.2	58.9	83.5	19.4	33.2
Mishima and Hibiki [64]	34.1	54.9	85.0	41.5	41.8	65.3	58.3	46.8	65.4
Yang and Webb [21]	40.3 [398]	37.2 [398]	59.5 [398]	34.6 [1781]	43.1 [1781]	76.4 [1781]	23.6 [789]	68.9 [789]	89.7 [789]
Yan and Lin [65]	247.9 [752]	19.8 [752]	27.7 [752]	173.3 [3056]	15.2 [3056]	26.3 [3056]	142.2 [1070]	20.9 [1070]	35.0 [1070]
Lee and Lee [66]	44.9	33.8	56.5	86.6	29.4	44.6	258.9	13.6	20.7
Chen et al. [67]	39.2	38.7	66.3	55.7	13.7	33.4	52.0	24.1	45.4
Hwang and Kim [39]	44.0 [1917]	31.4 [1917]	53.1 [1917]	37.4 [1541]	52.8 [1541]	71.3 [1541]	27.1 [333]	69.1 [333]	88.3 [333]
Sun and Mishima [68]	108.1	24.7	42.2	35.7	55.5	86.5	23.0	72.8	95.0
Li and Wu [69]	37.0	48.5	82.0	39.6 [3019]	58.6 [3019]	77.9 [3019]	40.8 [777]	49.8 [777]	69.5 [777]
Zhang et al. [70]	35.2 [2230]	52.6 [2230]	80.8 [2230]	39.7 [2252]	36.1 [2252]	67.0 [2252]	33.1 [552]	42.2 [552]	87.0 [552]
New correlation	25.7	67.5	92.3	23.7	70.8	93.7	17.5	85.0	99.2

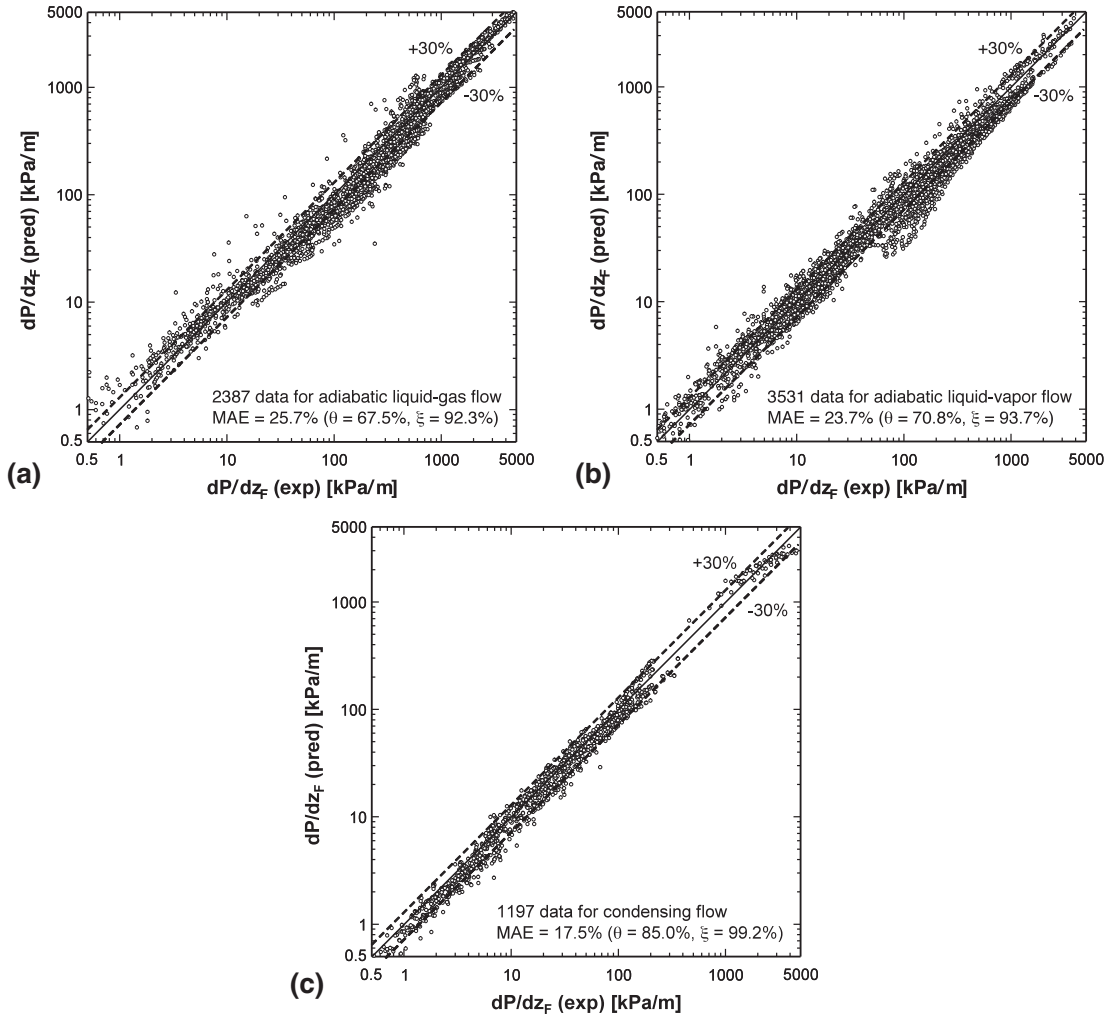

Fig. 8. Comparison of predictions of new correlation with three subsets of the consolidated database corresponding to: (a) adiabatic liquid–gas flow, (b) adiabatic liquid–vapor flow, and (c) condensing flow.

future work must pursue mechanistic, theoretical models that capture the important influences of small channel size. To achieve this goal, different models must be constructed for different flow regimes. For the annular condensation regime, models must address the important influence of interfacial waves. Past studies involving adiabatic, heated and evaporating liquid films have shown that waves can have a profound influence on mass, momentum and heat transfer in the film [15,92–98]. Another important issue is the dampening of turbulent fluctuations near the vapor–liquid interface due to surface tension forces [79,99]. Understanding these phenomena will require more sophisticated diagnostic techniques for measurement of annular film thickness and interfacial waves [98,100]. Similar efforts must also be pursued to both understand the interfacial instabilities responsible for the transition from annular to slug flow, and better describe the shape, size and motion of slug flow bubbles in pursuit of theoretical means for predicting pressure drop and heat transfer for slug flow.

6. Conclusions

A new universal approach to predicting two-phase frictional pressure drop for adiabatic and condensing mini/micro-channel flows is developed based on a consolidated database consisting of 7115 data points from 36 sources. The consolidated database is used to both assess the accuracy of prior models and correlations and develop the new universal correlation. Key findings from the study are as follows:

(1) Only a few prior models and correlations show relatively fair predictions of the consolidated database. These include the homogeneous equilibrium viscosity models of Dukler et al. [57] and Beattie and Whalley [58] and the macro-channel correlation by Müller-Steinhagen and Heck's [62]. However, the predictive capability of these models and correlations is compromised for specific subsets of the consolidated database.

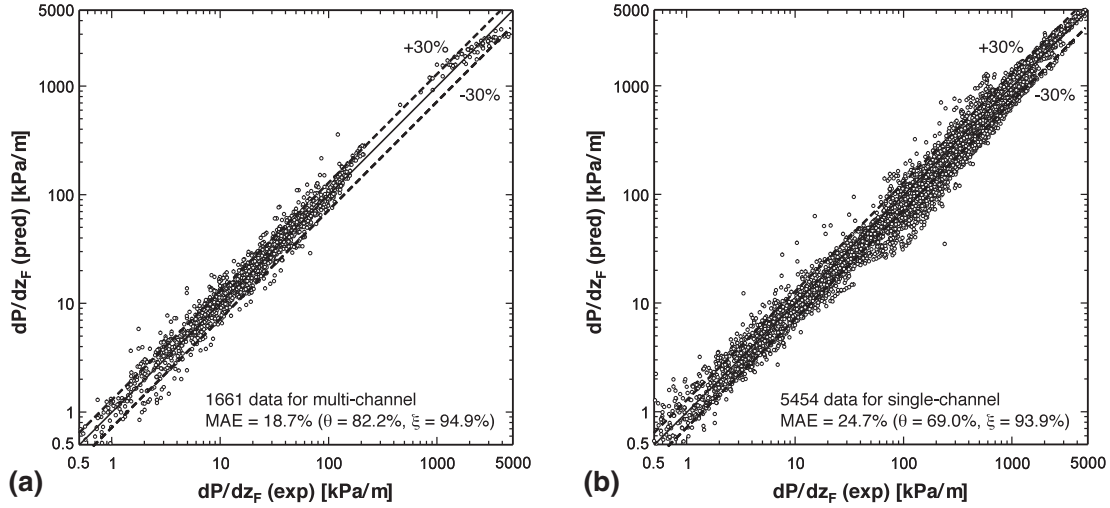

Fig. 9. Comparison of predictions of new correlation with two subsets of the consolidated database corresponding to: (a) multi-channels and (b) singlechannels.

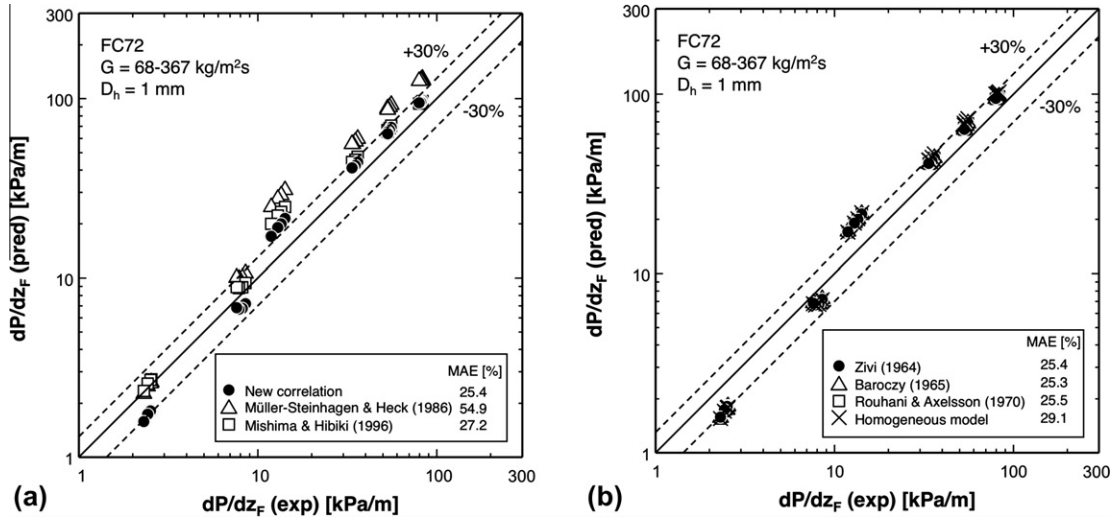

Fig. 10. (a) Comparison of FC72 experimental data [3] with predictions of the new and previous frictional pressure drop correlations, with the accelerational pressure gradient determined using the Zivi [60] void fraction relation. (b) Effect of void fraction relation used to determine the accelerational pressure gradient on the predictions of the new frictional pressure drop correlation.

(2) A new approach to predicting two-phase frictional pressure drop for adiabatic and condensing mini/micro-channel flows is proposed that accounts for the effects of small channel diameter by modifying the original Lockhart–Martinelli model with appropriate dimensionless parameters specific to each combination of liquid and vapor states. This approach provides excellent predictive capability against the entire consolidated database, with an overall MAE of 23.3%, and fairly uniform accuracy over broad ranges of all relevant parameters.

References

[1] I. Mudawar, Assessment of high-heat-flux thermal management schemes, IEEE Trans-CPMT: Comp. Packag. Technol. 24 (2001) 122–141.
[2] I. Mudawar, Two-phase micro-channel heat sinks: theory, applications and limitations, ASME J. Electron. Packag. 133 (2011) 041002-2.
[3] I. Mudawar, K.A. Estes, Optimizing and predicting CHF in spray cooling of a square surface, ASME J. Heat Transfer 118 (1996) 672–680.
[4] L. Lin, R. Ponnappan, Heat transfer characteristics of spray cooling in a closed loop, Int. J. Heat Mass Transfer 46 (2003) 3737–3746.
[5] J.R. Rybicki, I. Mudawar, Single-phase and two-phase cooling characteristics of upward-facing and downward-facing sprays, Int. J. Heat Mass Transfer 49 (2006) 5–16.
[6] Y. Katto, M. Kunihiro, Study of the mechanism of burn-out in boiling system of high burn-out heat flux, Bulletin JSME 16 (1973) 1357–1366.
[7] I. Mudawar, D.C. Wadsworth, Critical heat flux from a simulated electronic chip to a confined rectangular impinging jet of dielectric liquid, Int. J. Heat Mass Transfer 34 (1991) 1465–1480.
[8] D.C. Wadsworth, I. Mudawar, Enhancement of single-phase heat transfer and critical heat flux from an ultra-high-flux simulated microelectronic heat source to a rectangular impinging jet of dielectric liquid, ASME J. Heat Transfer 114 (1992) 764–768.
[9] M.E. Johns, I. Mudawar, An ultra-high power two-phase jet-impingement avionic clamshell module, ASME J. Electronic Packaging 118 (1996) 264–270.
[10] T.C. Willingham, I. Mudawar, Forced-convection boiling and critical heat flux from a linear array of discrete heat sources, Int. J. Heat Mass Transfer 35 (1992) 2879–2890.
[11] M.B. Bowers, I. Mudawar, High flux boiling in low flow rate, low pressure drop mini-channel and micro-channel heat sinks, Int. J. Heat Mass Transfer 37 (1994) 321–332.
[12] T.N. Tran, M.W. Wambsganss, D.M. France, Small circular- and rectangular-channel boiling with two refrigerants, Int. J. Multiphase Flow 22 (1996) 485–498.
[13] H.J. Lee, S.Y. Lee, Heat transfer correlation for boiling flows in small rectangular horizontal channels with low aspect ratios, Int. J. Multiphase Flow 27 (2001) 2043–2062.
[14] V. Khanikar, I. Mudawar, T. Fisher, Effects of carbon nanotube coating on flow boiling in a micro-channel, Int. J. Heat Mass Transfer 52 (2009) 3805–3817.
[15] S.M. Kim, J. Kim, I. Mudawar, Flow condensation in parallel micro-channels – Part 1: Experimental results and assessment of pressure drop correlations, Int. J. Heat Mass Transfer 55 (2012) 971–983.
[16] W. Qu, I. Mudawar, Transport phenomena in two-phase micro-channel heat sinks, ASME J. Electron. Packag. 126 (2004) 213–224.
[17] D.K. Hinde, M.K. Dobson, J.C. Chato, M.E. Mainland, N. Rhines, Condensation of refrigerants 12 and 134a in horizontal tubes with and without oil, University of Illinois at Urbana-Champaign (1992) ACRC TR-26.
[18] M.W. Wambsganss, J.A. Jendzejczky, D.M. France, N.T. Obot, Frictional pressure gradients in two-phase flow in a small horizontal rectangular channel, Exp. Thermal Fluid Sci. 5 (1992) 40–56.
[19] H. Fujita, T. Ohara, M. Hirota, H. Furuta, Gas–liquid flows in flat channels with small channel clearance, Adv. Multiphase Flow (1995) 441–451.
[20] H. Hirofumi, R.L. Webb, Condensation in Extruded Aluminum Tubes, Penn State Research Report, Showa Aluminum Corporation, 1995.
[21] C.Y. Yang, R.L. Webb, Friction pressure drop of R-12 in small hydraulic diameter extruded aluminum tubes with and without micro-fins, Int. J. Heat Mass Transfer 39 (1996) 801–809.
[22] K.A. Triplett, S.M. Ghiaasiaan, S.I. Abdel-Khalik, A. LeMouel, B.N. McCord, Gas-liquid two-phase flow in microchannels Part II: Void fraction and pressure drop, Int. J. Multiphase Flow 25 (1999) 395–410.
[23] Z.Y. Bao, D.F. Fletcher, B.S. Haynes, An experimental study of gas–liquid flow in a narrow conduit, Int. J. Heat Mass Transfer 43 (2000) 2313–2324.
[24] J.W. Coleman, Flow visualization and pressure drop for refrigerant phase change and air-water flow in small hydraulic diameter geometries, PhD Thesis, Iowa State University, IA, 2000.
[25] C.C. Wang, S.K. Chiang, Y.J. Chang, T.W. Chung, Two-phase flow resistance of refrigerants R-22, R-410A and R-407C in small diameter tubes, Trans. IChemE 79 (2001) 553–560.
[26] M. Zhang, R.L. Webb, Correlation of two-phase friction for refrigerants in small-diameter tubes, Exp. Thermal Fluid Sci. 25 (2001) 131–139.
[27] V.G. Nino, P.S. Hrnjak, T.A. Newell, Characterization of two-phase flow in microchannels, University of Illinois at Urbana-Champaign (2002) ACRC TR-202.
[28] D.C. Adams, P.S. Hrnjak, T.A. Newell, Pressure drop and void fraction in microchannels using carbon dioxide, ammonia, and R245fa as refrigerants, University of Illinois at Urbana-Champaign (2003) ACRC TR-221.
[29] C.A. Monroe, T.A. Newell, J.C. Chato, An experimental investigation of pressure drop and heat transfer in internally enhanced aluminum microchannels, University of Illinois at Urbana-Champaign (2003) ACRC TR-213.
[30] K.K. Pehlivan, Experimental study on two-phase flow regimes and frictional pressure drop in mini- and micro-channels, Concordia University, Canada, 2003. MS Thesis.
[31] J. Jang, P.S. Hrnjak, Condensation of CO2 at low temperature, University of Illinois at Urbana-Champaign (2004) ACRC CR-56.
[32] J.S. Shin, A study of flow condensation heat transfer inside mini-channels with new experimental techniques, PhD Thesis, Pohang University of Science and Technology, Korea, 2004.
[33] X. Tu, P.S. Hrnjak, Flow and heat transfer in microchannels 30 to 300 microns in hydraulic diameter, University of Illinois at Urbana-Champaign (2004) ACRC CR-53.
[34] A. Cavallini, D.D. Col, L. Doretti, M. Matkovic, L. Rossetto, C. Zilio, Two-phase frictional pressure gradient of R236ea, R134a, and R410A inside multi-port mini-channels, Exp. Thermal Fluid Sci. 29 (2005) 861–870.
[35] I.Y. Chen, C.L. Won, C.C. Wang, Influence of oil on R-410A two-phase frictional pressure drop in a small U-type wavy tube, Int. Comm. Heat Mass Transfer 32 (2005) 797–808.
[36] B. Mitra, Supercritical gas cooling and condensation of refrigerant R410A at near-critical pressures, PhD Thesis, Georgia Institute of Technology, GA, 2005.
[37] U.C. Andresen, Supercritical gas cooling and near-critical-pressure condensation of refrigerant blends in microchannels, PhD Thesis, Georgia Institute of Technology, GA, 2006.
[38] N.J. English, S.G. Kandlikar, An experimental investigation into the effect of surfactants on air-water two-phase flow in minichannels, Heat Transfer Eng. 27 (2006) 99–109.
[39] Y.W. Hwang, M.S. Kim, The pressure drop in microtubes and the correlation development, Int. J. Heat Mass Transfer 49 (2006) 1804–1812.
[40] R. Yun, J.H. Heo, Y. Kim, Evaporative heat transfer and pressure drop of R410A in microchannels, Int. J. Refrigeration 29 (2006) 92–100.
[41] B.S. Field, P.S. Hrnjak, Two-phase pressure drop and flow regime of refrigerants and refrigerant-oil mixtures in small channels, University of Illinois at Urbana-Champaign (2007) ACRC TR-261.
[42] C.Y. Park, P.S. Hrnjak, Carbon dioxide and R410A flow boiling heat transfer, pressure drop and flow pattern in horizontal tubes at low temperatures, University of Illinois at Urbana-Champaign (2007) ACRC TR-258.
[43] R. Revellin, J.R. Thome, Adiabatic two-phase frictional pressure drops in microchannels, Exp. Thermal Fluid Sci. 31 (2007) 673–685.
[44] J. Yue, G. Chen, Q. Yuan, L. Luo, Y. Gonthier, Hydrodynamics and mass transfer characteristics in gas-liquid flow through a rectangular microchannel, Chem. Eng. Sci. 62 (2007) 2096–2108.
[45] X. Quan, P. Cheng, H. Wu, An experimental investigation on pressure drop of steam condensing in silicon microchannels, Int. J. Heat Mass Transfer 51 (2008) 5454–5458.
[46] K. Dutkowski, Two-phase pressure drop of air-water in minichannels, Int. J. Heat Mass Transfer 52 (2009) 5185–5192.
[47] K.A. Marak, Condensation heat transfer and pressure drop for methane and binary methane fluids in small channels, PhD Thesis, Norwegian University of Science and Technology, Trondheim, 2009.
[48] C.Y. Park, P.S. Hrnjak, CO_2 flow condensation heat transfer and pressure drop in multi-port microchannels at low temperatures, Int. J. Refrigeration 32 (2009) 1129–1139.
[49] X. Huang, G. Ding, H. Hu, Y. Zhu, Y. Gao, B. Deng, Two-phase frictional pressure drop characteristics of R410A-oil mixture flow condensation inside 4.18mm and 1.6mm I.D. horizontal smooth tubes, HVAC&R Research 16 (2010) 453–470.
[50] C.W. Choi, D.I. Yu, M.H. Kim, Adiabatic two-phase flow in rectangular microchannels with different aspect ratios: Part I – Flow pattern, pressure drop and void fraction, Int. J. Heat Mass Transfer 54 (2011) 616–624.
[51] M. Ducoulombier, S. Colasson, J. Bonjour, P. Haberschill, Carbon dioxide flow boiling in a single microchannel – Part I: Pressure drops, Exp. Thermal Fluid Sci. 35 (2011) 581–596.
[52] C.B. Tibirica, G. Ribatski, Two-phase frictional pressure drop and flow boiling heat transfer for R245fa in a 2.32-mm tube, Heat Transfer Eng. 32 (2011) 1139–1149.
[53] W.H. McAdams, W.K. Woods, L.C. Heroman, Vaporization inside horizontal tubes, II. Benzene-oil mixture, Trans. ASME 64 (1942) 193–200.
[54] W.W. Akers, H.A. Deans, O.K. Crosser, Condensing heat transfer within horizontal tubes, Chem. Eng. Prog. 54 (1958) 89–90.
[55] A. Cicchitti, C. Lombardi, M. Silvestri, G. Soldaini, R. Zavalluilli, Two-phase cooling experiments-pressure drop, heat transfer and burnout measurements, Energia nucleare 7 (1960) 407–425.
[56] W.L. Owens, Two-phase pressure gradient. Int. Dev. Heat Transfer, Pt. II., ASME, New York, 1961.
[57] A.E. Dukler, M. Wicks, R.G. Cleaveland, Pressure drop and hold up in two-phase flow, AIChE J. 10 (1964) 38–51.
[58] D.R.H. Beattie, P.B. Whalley, A simple two-phase frictional pressure drop calculation method, Int. J. Multiphase Flow 8 (1982) 83–87.
[59] S. Lin, C.C.K. Kwok, R.Y. Li, Z.H. Chen, Z.Y. Chen, Local frictional pressure drop during vaporization of R-12 through capillary tubes, Int. J. Multiphase Flow 17 (1991) 95–102.

[60] R.W. Lockhart, R.C. Martinelli, Proposed correlation of data for isothermal two-phase, two-component flow in pipes, Chem. Eng. Prog. 45 (1949) 39–48.
[61] L. Friedel, Improved friction pressure drop correlations for horizontal and vertical two-phase pipe flow, European Two-phase Group Meeting, Ispra, Italy, (1979) Paper E2.
[62] H. Müller-Steinhagen, K. Heck, A simple friction pressure drop correlation for two-phase flow in pipes, Chem. Eng. Process. 20 (1986) 297–308.
[63] C.C. Wang, C.S. Chiang, D.C. Lu, Visual observation of two-phase flow pattern of R-22, R-134a, and R-407C in a 6.5-mm smooth tube, Exp. Thermal Fluid Sci. 15 (1997) 395–405.
[64] K. Mishima, T. Hibiki, Some characteristics of air–water two-phase flow in small diameter vertical tubes, Int. J. Multiphase Flow 22 (1996) 703–712.
[65] Y.Y. Yan, T.F. Lin, Condensation heat transfer and pressure drop of refrigerant R-134a in a small pipe, Int. J. Heat Mass Transfer 42 (1999) 697–708.
[66] H.J. Lee, S.Y. Lee, Pressure drop correlations for two-phase flow within horizontal rectangular channels with small heights, Int. J. Multiphase Flow 27 (2001) 783–796.
[67] I.Y. Chen, K.S. Yang, Y.J. Chang, C.C. Wang, Two-phase pressure drop of air-water and R-410A in small horizontal tubes, Int. J. Multiphase Flow 27 (2001) 1293–1299.
[68] L. Sun, K. Mishima, Evaluation analysis of prediction methods for two-phase flow pressure drop in mini-channels, Int. J. Multiphase Flow 35 (2009) 47–54.
[69] W. Li, Z. Wu, A general correlation for adiabatic two-phase pressure drop in micro/mini-channels, Int. J. Heat Mass Transfer 53 (2010) 2732–2739.
[70] W. Zhang, T. Hibiki, K. Mishima, Correlations of two-phase frictional pressure drop and void fraction in mini-channel, Int. J. Heat Mass Transfer 53 (2010) 453–465.
[71] I. Mudawar, A.H. Howard, C.O. Gersey, An analytical model for near-saturated pool boiling CHF on vertical surfaces, Int. J. Heat Mass Transfer 40 (1997) 2327–2339.
[72] A.H. Howard, I. Mudawar, Orientation effects on pool boiling CHF and modeling of CHF for near-vertical surfaces, Int. J. Heat Mass Transfer 42 (1999) 1665–1688.
[73] J.E. Galloway, I. Mudawar, CHF mechanism in flow boiling from a short heated wall-Part 1. Examination of near-wall conditions with the aid of photomicrography and high-speed video imaging, Int. J. Heat Mass Transfer 36 (1993) 2511–2526.
[74] J.E. Galloway, I. Mudawar, CHF mechanism in flow boiling from a short heated wall-Part 2. Theoretical CHF model, Int. J. Heat Mass Transfer 36 (1993) 2527–2540.
[75] C.O. Cersey, I. Mudawar, Effects of heater length and orientation on the trigger mechanism for near-saturated flow boiling critical heat flux – I. Photographic study and statistical characterization of the near-wall interfacial features, Int. J. Heat Mass Transfer 38 (1995) 629–641.
[76] C.O. Cersey, I. Mudawar, Effects of heater length and orientation on the trigger mechanism for near-saturated flow boiling critical heat flux – II. Critical heat flux model, Int. J. Heat Mass Transfer 38 (1995) 643–654.
[77] J.C. Sturgis, I. Mudawar, Critical heat flux in a long, rectangular channel subjected to onesided heating – I. Flow visualization, Int. J. Heat Mass Transfer 42 (1999) 1835–1847.
[78] J.C. Sturgis, I. Mudawar, Critical heat flux in a long, rectangular channel subjected to onesided heating – II. Analysis of critical heat flux data, Int. J. Heat Mass Transfer 42 (1999) 1849–1862.
[79] S.M. Kim, I. Mudawar, Theoretical model for annular flow condensation in rectangular micro-channels, Int. J. Heat Mass Transfer 55 (2012) 958–970.
[80] I. Mudawar, M.B. Bowers, Ultra-high critical heat flux (CHF) for subcooled water flow boiling – I. CHF data and parametric effects for small diameter tubes, Int. J. Heat Mass Transfer 42 (1999) 1405–1428.
[81] D.D. Hall, I. Mudawar, Ultra-high critical heat flux (CHF) for subcooled water flow boiling – II. High-CHF database and design parameters, Int. J. Heat Mass Transfer 42 (1999) 1429–1456.
[82] D.D. Hall, I. Mudawar, Critical heat flux (CHF) for water flow in tubes – I. Compilation and assessment of world CHF data, Int. J. Heat Mass Transfer 43 (2000) 2573–2604.
[83] D.D. Hall, I. Mudawar, Critical heat flux (CHF) for water flow in tubes – II. Subcooled CHF correlations, Int. J. Heat Mass Transfer 43 (2000) 2605–2640.
[84] S.M. Zivi, Estimation of steady-state steam void-fraction by means of the principle of minimum entropy production, ASME J. Heat Transfer 86 (1964) 247–252.
[85] F.P. Incropera, D.P. Dewitt, Fundamentals of Heat and Mass Transfer, 5th ed., Wiley, New York, 2002.
[86] R.K. Shah, A.L. London, Laminar flow forced convection in ducts: a source book for compact heat exchanger analytical data, Academic press, New York, 1978 (Supl 1).
[87] A. Agarwal, Heat transfer and pressure drop during condensation of refrigerants in microchannels, PhD Thesis, Georgia Institute of Technology, GA, 2006.
[88] T. Bohdal, H. Charun, M. Sikora, Comparative investigations of the condensation of R134a and R404A refrigerants in pipe minichannels, Int. J. Heat Mass Transfer 54 (2011) 1963–1974.
[89] C.J. Baroczy, Correlation of liquid fraction in two-phase flow with applications to liquid metals, Chem. Eng. Prog. 61 (1965) 179–191.
[90] S.Z. Rouhani, E. Axelsson, Calculation of void volume fraction in the subcooled and quality boiling region, Int. J. Heat Mass Transfer 13 (1970). 393-393.
[91] E.W. Lemmon, M.L. Huber, M.O. McLinden, Reference fluid thermodynamic and transport properties – REFPROP Version 8.0, NIST, MD, 2007.
[92] S.M. Kim, I. Mudawar, Flow condensation in parallel micro-channels – Part 2: Heat transfer results and correlation technique, Int. J. Heat Mass Transfer 55 (2012) 984–994.
[93] J.A. Shmerler, I. Mudawar, Local heat transfer coefficient in wavy free-falling turbulent liquid films undergoing uniform sensible heating, Int. J. Heat Mass Transfer 31 (1988) 67–77.
[94] J.A. Shmerler, I. Mudawar, Local evaporative heat transfer coefficient in turbulent free-falling liquid films, Int. J. Heat Mass Transfer 31 (1988) 731–742.
[95] T.H. Lyu, I. Mudawar, Statistical investigation of the relationship between interfacial waviness and sensible heat transfer to a falling liquid film, Int. J. Heat Mass Transfer 34 (1991) 1451–1464.
[96] T.H. Lyu, I. Mudawar, Determination of wave-induced fluctuations of wall temperature and convective heat transfer coefficient in the heating of a turbulent falling liquid film, Int. J. Heat Mass Transfer 34 (1991) 2521–2534.
[97] I. Mudawar, R.A. Houpt, Mass and momentum transport in Falling liquid films laminarized at relatively high Reynolds numbers, Int. J. Heat Mass Transfer 36 (1993) 3437–3448.
[98] I. Mudawar, R.A. Houpt, Measurement of mass and momentum transport in wavy-laminar falling liquid films, Int. J. Heat Mass Transfer 36 (1993) 4151–4162.
[99] I. Mudawar, M.A. El-Masri, Momentum and heat transfer across freely-falling turbulent liquid films, Int. J. Multiphase Flow 12 (1986) 771–790.
[100] J.E. Koskie, I. Mudawar, W.G. Tiederman, Parallel-wire probes for measurement of thick liquid films, Int. J. Multiphase Flow 15 (1989) 521–530.